

Noise Distribution Decomposition based Multi-Agent Distributional Reinforcement Learning

Wei Geng, Baidi Xiao, Rongpeng Li, Ning Wei, Dong Wang, and Zhifeng Zhao



Abstract—Generally, Reinforcement Learning (RL) agent updates its policy by repetitively interacting with the environment, contingent on the received rewards to observed states and undertaken actions. However, the environmental disturbance, commonly leading to noisy observations (e.g., rewards and states), could significantly shape the performance of agent. Furthermore, the learning performance of Multi-Agent Reinforcement Learning (MARL) is more susceptible to noise due to the interference among intelligent agents. Therefore, it becomes imperative to revolutionize the design of MARL, so as to capably ameliorate the annoying impact of noisy rewards. In this paper, we propose a novel decomposition-based multi-agent distributional RL method by approximating the globally shared noisy reward by a Gaussian mixture model (GMM) and decomposing it into the combination of individual distributional local rewards, with which each agent can be updated locally through distributional RL. Moreover, a diffusion model (DM) is leveraged for reward generation in order to mitigate the issue of costly interaction expenditure for learning distributions. Furthermore, the optimality of the distribution decomposition is theoretically validated, while the design of loss function is carefully calibrated to avoid the decomposition ambiguity. We also verify the effectiveness of the proposed method through extensive simulation experiments with noisy rewards. Besides, different risk-sensitive policies are evaluated in order to demonstrate the superiority of distributional RL in different MARL tasks.

Index Terms—Multi-agent reinforcement learning, noisy environment, distributional reinforcement learning, distribution decomposition, diffusion model.

1 INTRODUCTION

REINFORCEMENT learning (RL) [53] has significant applications in various domains, including game AI training [29], robot control [47], and large language models' optimization [15]. With the rise of Deep Learning (DL) [30] technology and its remarkable achievements in various fields, the integration of deep neural networks (DNNs) and RL [21] has become a hot topic in research. The accompanied tremendous success of DRL has prompted researchers to shift their focus to the field of Multi-Agent Systems

(MAS) [14], and given rise to Multi-Agent Reinforcement Learning (MARL). For most cooperative MARL tasks, it is crucial to develop appropriate means to leverage a global reward to train decentralized action value (i.e., Q -value) or state value (i.e., V -value) networks, and update the policies accordingly, especially for settings with partial observations and constrained communications [25], [52]. In particular, some value decomposition methods [40], [41], [49], [52] are proposed.

Nevertheless, environmental noise widely exists in practice due to internal and external factors (e.g., electronic noise from sensors, the influences of temperature, pressure and illumination) [27], and most RL algorithms are vulnerable in noisy scenarios with unstable performance [56]. Some off-the-shelf MARL algorithms also face troublesome converging issues and experience severely deteriorated performance under noisy scenarios, especially for those adversarial tasks where agents might possibly suffer malicious interference from opponents [28]. The distributional RL [1], which models the Q -value or state value as a distribution, emerges as a promising solution for anti-noise. However, incorporating value decomposition into classic distributional RL for noisy MARL tasks is rather counter-effective, considering the multi-folded detrimental effects. Firstly, it is typically hard to train a quantile network [1], [8], which aims to learn a specific Cumulative Distribution Function (CDF) of Q -value or state value function. Therefore, it usually takes distributional RL algorithms more time to converge. Secondly, making specific assumptions about the exact type of the global distribution lacks robustness. As not all types of distribution are additive or support linear operations, changing the types of individual distributions through temporal-difference (TD) update also increases model complexity [34]. Additionally, decomposing the global distribution into individual distributions is erratic and unstable [51], as slight changes of the global distribution usually cause individual distributions to vibrate drastically. Finally, the interaction cost between agents and the environment, as well as the learning cost, will significantly increase [4].

In this paper, we propose the brand new Noise Distribution Decomposition (NDD) MARL method, wherein the ideas of distributional RL and value decomposition are jointly leveraged to ameliorate the flexibility of distributed

W. Geng is with Hangzhou Institute for Advanced Study, UCAS (email: gengwei21@mailsucas.ac.cn).

B. Xiao and R. Li are with College of Information Science and Electronic Engineering, Zhejiang University (email: {xiaobaidi, lirongpeng}@zju.edu.cn).

D. Wang is with Research Institute of China Telecom (email: wangd5@chinatelecom.cn).

N. Wei and Z. Zhao are with Zhejiang Lab (email: {weining, zhaozf}@zhejianglab.com).

agents to noisy rewards. The utilization of distributional RL enables agent to remap quantiles using distortion risk function, thereby better taking account of the distribution over returns and potentially generating distinctive policies with different risk-sensitive functions [8]. Meanwhile, in order to tackle the difficulties to incorporate value decomposition into classic distributional RL for MARL tasks, we successfully leverage a parametric Gaussian Mixture Model (GMM) [42] and establish a viable decomposition means with calibrated Wasserstein-metric-based [9] loss function. Furthermore, inspired by the astonishing representation capabilities of Diffusion Models (DM) [12], [22], [37], [39], [44], we also incorporate DM to model the noise distribution, so as to reduce the interaction cost. The main contributions of our work can be summarized as follows:

- We introduce NDD on top of distributional RL and value decomposition in MARL. For the ensemble of agents, NDD approximates the distribution of the noisy global reward by GMM, and obtains the local distributional value functions indirectly for yielding more stable individual policies. For a single agent, NDD also contributes to more conveniently learning the Q -value distribution even with partial observation.
- We extend distributional RL to the multi-agent domain and introduce distortion risk functions, which facilitate the determination to adopt adventurous or conservative strategies by adjusting Q -value distributions, so as to provide more flexibility than traditional RL with expectation.
- We carefully calibrate a Wasserstein-metric-based loss function to learn the accurate distributional value function corresponding to each agent and prove the consistency between the globally optimal action and locally optimal actions theoretically.
- In order to alleviate the high cost of environment interaction required for learning distributions, we introduce DM to augment the data for solving the data scarcity, and prove the bounded expectations of the generation and approximation error in the augmented data.

In the rest of this paper, we present the related work of RL and MARL in Section 2. Afterwards, based on the necessary notations and preliminaries in Section 3, we describe our proposed method in Section 4. Subsequently, numerous simulation results are shown to validate the effectiveness and superiority of our method in Section 5. Finally, Section 6 concludes the paper.

2 RELATED WORK

According to the cooperativeness between their reward functions, MARL can be categorized into three types (i.e., fully cooperative, fully competitive, and mix tasks) [5]. For fully cooperative tasks, the reward functions of agents are identical, signifying that all agents are striving to achieve a common goal [18], [59]. Algorithms targeted at this type of tasks can integrate computational and learning capabilities of MAS, and potentially achieve gains beyond simple summation [5]. For fully competitive tasks, the reward

functions are opposite, typically involving two completely antagonistic agents in the environment, while the agents aim to maximize their own rewards and minimize the opponent’s rewards, with Minimax-Q [32] being a representative algorithm. In mixed tasks, the relationship of agents could be stochastic, leading to complicated reward functions of agents and making this model suitable for self-interested agents [5]. Generally, the resolution of such tasks is often associated with the concept of equilibrium in game theory. In this paper, we primarily focus the first fully cooperative setting, since the related algorithms we will mention next are more conducive to implementation, migration, and expansion to more large-scale MAS [5], [55] compared with other two types. On the other hand, cooperative algorithm has a close connection with distributed optimization [55]. Therefore, efficient optimization techniques such as decentralized training, asynchronous training [62], communication learning [17], [50] can be introduced to tackle issues in cooperative learning.

However, there are still many unresolved issues for cooperative algorithms. First, in a multi-agent environment, each agent not only needs to consider its own actions and rewards, but also must take account of the influences of the actions undertaken by other agents [5]. Such an intricate process of interaction and interconnection results in constantly undergoing changes of a non-stationary environment, making the actions and strategy choices among agents inter-dependent. Therefore, due to the updated strategies of other agents, it impedes each agent to approximate accurate Q -value or state value functions for making an self-optimized strategy. To solve this issue, based on Deep Q-Network (DQN) [35], Castaneda *et al.* [6] propose to modify the value functions and reward functions to fit the inter-dependence among agents. Diallo *et al.* [13] introduce a parallel computing mechanism into DQN to expedite the convergence in non-stationary environments. Foerster *et al.* [17] focus on improving the experience replay to better adapt to continuously changing non-stationary environments. Another important issue in cooperative MARL lies in the limitation of partial observation. That is, agents can only make near-optimal decisions based on their own partially observable information. In the collaborative task with local observations and globally shared rewards, value decomposition methods are often adopted to effectively learn the different contributions of agents from global rewards. For example, VDN [52] decomposes the global value function into the sum of individual value functions. Based on VDN, QMIX [41] further generalizes the way of value decomposition through sophisticated transformation, and puts forward an important assumption on the monotonicity of the global Q -value function with respect to local Q -value functions. Focusing on the further exploration of the joint action, Weighted QMIX [40] and QTRAN [49] discuss the relationship between individual optimal actions and the global optimal joint action. Nevertheless, all these value decomposition algorithms [40], [41], [49], [52] suffer from the adoption of over-simplistic expectation operation, which is not sufficient to describe noisy environment that agents may encounter. In a nutshell, it necessitates the more comprehensive characterization of the environment and develop novel decomposition means to explore adventurous

or conservative strategies. Coincidentally, it falls into the scope of distributional RL [1], [8], [9] and distortion risk functions [8].

Primarily adopted in single-agent settings, Distributional RL [1], [8], [9] comprehensively characterizes the fluctuation by replacing the expectation of state values or Q -values with the corresponding distributions. For example, DFAC [51] extends value decomposition method to the field of distributional RL, and develops the joint quantile function decomposition to extend VDN and QMIX to DDN and DMIX on condition of stable and noise-free rewards. But, a noticeable drawback of distributional RL is the increased computation and interaction cost to train quantile networks alongside the TD update. For combatting the computation cost, DRE-MARL [24] designs the multi-action-branch reward estimation and policy-weighted reward aggregation for stabilized training. Furthermore, distortion risk functions, which primarily adjust the risk preference of policy in the Q -value distribution and are mainly employed in tasks where the correlation between risk and reward is evident, are proposed by [8]. Despite the progress in single-agent setting, the adoption of distortion risk functions is worthy further investigation, as it may disrupt the collaboration among MAS in MARL and convergence issues may arise if theoretical guarantees lack [8], [51]. Meanwhile, the interaction cost can be compensated by generative models [23], [58]. Among them, DM [22] is renowned for its astonishing capability in the fields of image synthesis [12], image inpainting, color restoration, image decompression [44] and text-to-image [37], [39]. RL has reaped benefits of DMs with significant improvement in cross-task learning and experience augmentation. For example, [60] and [20] use DM for policy generation in single agent tasks. J. Geng [19] leverages DM to encapsulate policies within MAS context, thereby fostering efficient and expressive inter-agent coordination. DOM2 [31] incorporates DM into the policy network and proposes a trajectory-based data-augmentation scheme in training. However, mostly in single-agent settings, these studies lack the validation in non-stationary and noisy environments. Moreover, the approximation errors of DM in generating samples also lack theoretical analyses.

3 BACKGROUND AND PRELIMINARIES

This section mainly discusses the base model in our work and the formulations of relevant methods. The main notations used in this paper are listed in Table 1.

3.1 Preliminaries

A cooperative multi-agent task can be described as the decentralized partially observable Markov decision process (Dec-POMDP), consisting of a tuple $\langle \mathcal{S}, \mathcal{A}, \mathcal{P}, \mathcal{R}, \mathcal{O}, \Omega, \mathcal{I}, \gamma \rangle$ [38], [41]. Specifically, $s \in \mathcal{S}$ denotes the global state and $\mathbf{a} = [a^{[1]}, \dots, a^{[N]}] \in \mathcal{A}$ is the joint action of N agents. The joint action causes a transition from current state s to next state s' according to the transition function $\mathcal{P}(s'|s, \mathbf{a}) : \mathcal{S} \times \mathcal{A} \times \mathcal{S} \rightarrow [0, 1]$. Specially, all agents share a global reward function $\mathcal{R}(s, \mathbf{a}) : \mathcal{S} \times \mathcal{A} \rightarrow \mathbb{R}$, whose output is $R \sim \mathcal{D}$. And r is sample from R . Each agent

TABLE 1
Main Notations Used in This Paper.

Notation	Definition
N	Number of agents
\mathcal{I}	Set of agents
\mathcal{S}, \mathcal{A} , and \mathcal{O}	The state, joint action and observation space
s	Global state
$\mathbf{a} = [a^{[1]}, \dots, a^{[N]}]$	Joint action of all agents
$\mathbf{o} = [o^{[1]}, \dots, o^{[N]}]$	Joint observation of all agents
Q and V	action value and state value function
$\mathbf{w} = [w^{[1]}, \dots, w^{[N]}]^\top$	Joint weight vector of all agents
μ_i, σ_i	Mean and standard deviation related to agent i
$\boldsymbol{\pi} = [\pi^{[1]}, \dots, \pi^{[N]}]$	Joint policy of all agents
$\theta^{[1]}, \dots, \theta^{[N]}$	Neural network parameters of all agents
Z	Random variable fitting Q -value distribution
F_Z	CDF of random variable Z
τ	Quantile value of a target distribution
$\rho(\tau)$	Distortion risk function about quantile τ
γ	Discount factor
R	Random variable fitting reward distribution
r and \mathcal{R}	Reward sample produced by the function \mathcal{R}
$r^{<k>}$	Generated reward in k -th step of DM
K	Total diffusion steps of DM
v_1, \dots, v_K and $\omega_1, \dots, \omega_K$	Predefined hyper-parameters in K steps of DM
Θ	Parameters of DM
$\mathcal{D}_q(\cdot)$	Distribution of random variable or its sample
G	Discounted accumulated global reward
d_p	Wasserstein distance computed by L_p -norm
\mathcal{D}	Global reward distribution
$\hat{\mathcal{D}}_l$	Decomposed distribution of local reward

$i \in \mathcal{I} \equiv \{1, \dots, N\}$ draws individual observations $o^{[i]} \in \mathcal{O}$ according to the observation function $\Omega(s, i) : \mathcal{S} \times \mathcal{I} \rightarrow \mathcal{O}$. Besides, $\gamma \in [0, 1)$ is a discount factor. Within the framework of Dec-POMDP, a joint policy $\boldsymbol{\pi}$ is corresponded to a joint Q -value function as

$$Q^\pi(s_t, \mathbf{a}_t) = \mathbb{E}_{s_{t+1:\infty}, \mathbf{a}_{t+1:\infty}} [G_t | s_t, \mathbf{a}_t, \boldsymbol{\pi}], \quad (1)$$

where $G_t = \sum_{m=0}^{\infty} \gamma^m \mathcal{R}(s_{t+m}, \mathbf{a}_{t+m})$. $Z^\pi(s_t, \mathbf{a}_t)$ is Q -value distribution with $\mathbb{E}[Z^\pi(s_t, \mathbf{a}_t)] = Q^\pi(s_t, \mathbf{a}_t)$. F_Z is CDF of $Z^\pi(s_t, \mathbf{a}_t)$ and τ is CDF's output, which can be distorted by distortion risk function $\rho(\tau)$. DM gradually adds Gaussian noises to sample r from \mathcal{D} by K times and then reconstructs it in reverse. In the diffusion process,

$r^{<k>} \sim \mathcal{D}_q(r^{<k>})$ is a generated sample in k -th step, $k \in [0, \dots, K]$, where $\mathcal{D}_q(\cdot)$ represents the distribution of the corresponding sample. The details of distortion risk functions and DM shall be given in Section 3.5 and Section 3.6, respectively.

3.2 Problem Formulation

In this paper, we primarily consider N RL agents (i.e., a group of RL-empowered distributed robots equipped with intelligent sensing devices and basic computing power) to perform certain cooperative tasks as shown in Fig. 1. Consistent with the general settings in Dec-POMDP, at each time-step t , agent i capably utilizes on-board sensors to access to a partial environmental observation $o_t^{[i]} \in \mathcal{O}$. Observations may include partial states of some teammates, received messages, or the relative positions to certain target points. This often depends on the specific task executed by the whole team. Notably, in this paper, we assume that the state s and the environmental observations $\mathbf{o} = [o^{[1]}, \dots, o^{[N]}]$ are equivalent. With a DM for data augmentation, every agent attempts to learn Q -value distributions and remaps them with distortion risk functions for yielding policy corresponding to different tasks. Based on the observation $o_t^{[i]}$, agent i responds with action $a_t^{[i]}$ (i.e., movement direction and message exchange) according to its policy $\pi^{[i]}(a_t^{[i]}|o_t^{[i]})$. Afterwards, the environmental state transits from s_t to next state s_{t+1} according to the transition function $\mathcal{P}(s_{t+1}|s_t, \mathbf{a}_t)$. Meanwhile, other observations and global information can be used for the calculation of reward from $\mathcal{R}(s_t, \mathbf{a}_t)$ by a suitable ‘‘virtual’’ agent (e.g., a centralized server or a computing-capable global-oriented robot). Notably, since the observation provided by sensors, or exactly the reward, could be polluted by internal or external noise, we formulate the reward by a random variable $R \sim \mathcal{D}$. In the subsequent sections, targeted at the aforementioned MARL settings, we mainly discuss how to apply our method NDD to tackle the noisy rewards, so as to maximize the average reward of episodes for the entire team.

3.3 Value Decomposition

Value decomposition methods [40], [41], [49], [52] belong to one of the typical methods to learn decentralized Q -value networks from globally shared rewards. As one of the pioneering works of value decomposition, QMIX [41] holds that under a monotonicity constraint, the joint of individually optimal actions is equivalent to the optimal joint action in regard to the Q -value function, which is also a crucial criteria for MARL with distributed deployment of agents. That is,

$$\underset{\mathbf{a}}{\operatorname{argmax}} Q_{\text{global}}(\mathbf{o}, \mathbf{a}) = \left(\begin{array}{c} \underset{a^{[1]}}{\operatorname{argmax}} Q_1(o^{[1]}, a^{[1]}) \\ \vdots \\ \underset{a^{[N]}}{\operatorname{argmax}} Q_N(o^{[N]}, a^{[N]}) \end{array} \right), \quad (2)$$

where $Q_{\text{global}}(\mathbf{o}, \mathbf{a})$ indicates the joint Q -value function of all agents and $Q_i(o^{[i]}, a^{[i]})$ is the Q -value function corre-

sponding to agent i . Besides, the monotonicity constraint can be formally written as

$$\frac{\partial Q_{\text{global}}(\mathbf{o}, \mathbf{a})}{\partial Q_i(o^{[i]}, a^{[i]})} \geq 0, \quad \forall i = 1, 2, \dots, N. \quad (3)$$

Furthermore, in order to satisfy (3), a mixing network is proposed to combine $Q_i(o^{[i]}, a^{[i]})$ into $Q_{\text{global}}(\mathbf{o}, \mathbf{a})$ with non-linear transformation.

3.4 Distributional RL

Distributional RL [1] aims to learn the distribution of Q -value or state value, so as to capture the more comprehensive information of random rewards (i.e., noisy rewards that follow a specific distribution). Besides, distributional RL benefits agents to hold different risk tendencies (e.g., risk-averse and risk-seeking) to choose preferred policies [8]. Specially for multi-agent distributional RL, given the state s and joint action \mathbf{a} , the transition operator P^π is defined as

$$P^\pi Z(s, \mathbf{a}) \stackrel{D}{:=} Z(S', \mathbf{A}'), \quad (4)$$

where the operator $U \stackrel{D}{:=} V$ indicates that the random variable U is distributed according to the same law as V . $Z(s, \mathbf{a})$ denotes the action value distribution with the expectation $Q(s, \mathbf{a})$, and capital letters S' and \mathbf{A}' are used to emphasize the random nature of next state-action pair (i.e., $S' \sim \mathcal{P}(\cdot|s, \mathbf{a})$ and $\mathbf{A}' \sim \pi(\cdot|S')$). On this basis, the distributional Bellman operator \mathcal{T}^π [1] is defined as:

$$\mathcal{T}^\pi Z(s, \mathbf{a}) \stackrel{D}{:=} R(s, \mathbf{a}) + \gamma P^\pi Z(s, \mathbf{a}). \quad (5)$$

That is to say, $Z(s, \mathbf{a})$, which describes the distribution of Q -value, is characterized by the interaction of three random variables (i.e., the reward $R(s, \mathbf{a})$, the next pair of state-action (S', \mathbf{A}') and the corresponding $Z(S', \mathbf{A}')$ according to (4)). In distributional RL, (5) is used to update $Z(s, \mathbf{a})$ with next state and action by temporal difference.

Accordingly, on account of the globally shared noisy reward and partial observation, (1) can be rewritten as

$$Z_{\text{global}}^\pi(\mathbf{o}, \mathbf{a}) = \sum_{t=0}^{\infty} \gamma^t R(\mathbf{o}_t, \mathbf{a}_t), \quad (6)$$

where $\pi = [\pi^{[1]}, \dots, \pi^{[N]}]$ denotes the joint policy of all agents. As mentioned in Section 3.2, $R(\mathbf{o}_t, \mathbf{a}_t)$ is a random variable of the noisy reward following an arbitrary distribution \mathcal{D} , which can be approximately regarded as a GMM and decomposed into N Gaussian components.

On the other hand, it is critical to measure the distributional difference between the true distribution of noisy reward and the approximated one. In this regard, Wasserstein metric [9] can be leveraged and mathematically defined as

$$d_p(F, G) = \left(\int_0^1 |F^{-1}(u) - G^{-1}(u)|^p du \right)^{\frac{1}{p}}, \quad (7)$$

where F and G are the CDFs of random variables U and V , respectively. $p < \infty$ implies to take an L_p norm for this metric. Furthermore, in single-agent settings, some robust approaches have been proposed by using quantile to evaluate and then fit the Q -value distribution [8], [9].

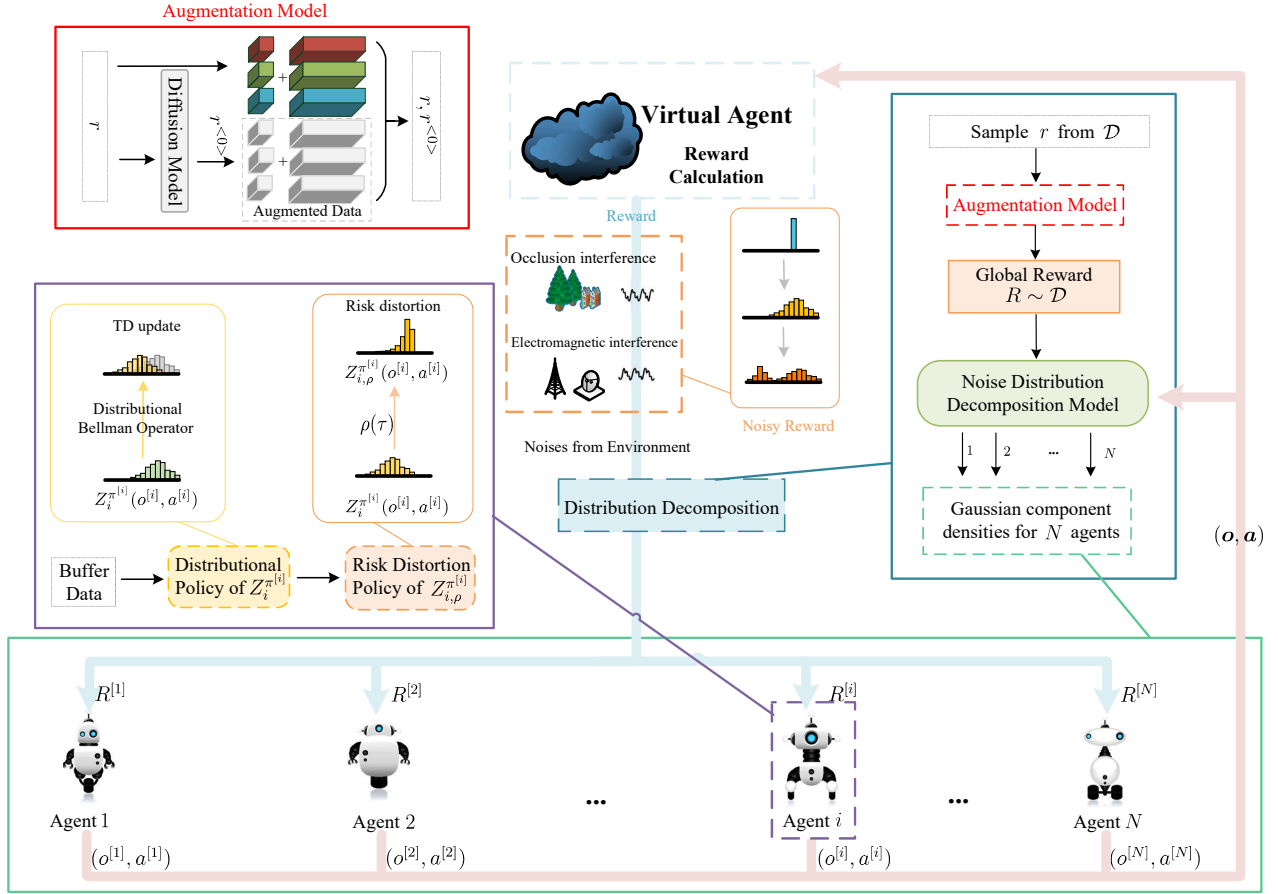


Fig. 1. The framework of NDD-based cooperative multi-agent distributional RL with noisy rewards.

3.5 Distortion Risk Function

Intuitively, the action corresponding to the maximum expectation value like Q -value does not always mean the optimal decision under particular scenarios. Therefore, different risk strategies, which expand the class of policies on account of the distributions over returns [8], are applicable to different task scenarios using distributional RL, and often reflect the underlying risk associated with certain actions.

Moreover, $\rho(\tau) : [0, 1] \rightarrow [0, 1]$ is defined as a distortion risk measure, where τ is typically used to represent the quantile of F_Z . Then, the distorted Q -value function $Q_\rho(\mathbf{o}, \mathbf{a})$ can be expressed in terms of $\rho(\tau)$ as

$$Q_\rho(\mathbf{o}, \mathbf{a}) = \mathbb{E}[Z_\rho(\mathbf{o}, \mathbf{a})] = \int z d\rho[F_Z(z)]. \quad (8)$$

Dabney *et al.* [8] introduce a parameter η to make $\rho(\tau)$ more flexible and adaptable, and further present the following four functions based on human decision-making habits and optimization costs.

$$(1) \quad \rho_\eta(\tau) = \text{CPW}(\eta, \tau) = \frac{\tau^\eta}{(\tau^\eta + (1 - \tau)^\eta)^{\frac{1}{\eta}}}. \quad (9)$$

The CPW is the cumulative probability weighting parameterization proposed in cumulative prospect theory [54]. It can be observed η is locally concave for small values of τ , while convex for larger values

of τ . Actually, concavity corresponds to risk-averse and convexity to risk-seeking policies [61]. [61] recommends $\eta = 0.71$.

$$(2) \quad \rho_\eta(\tau) = \text{WANG}(\eta, \tau) = \Phi(\Phi^{-1}(\tau) + \eta). \quad (10)$$

WANG is proposed in [57] where Φ and Φ^{-1} are taken to be the standard CDF of Normal distribution and its inverse. Intuitively, it produces risk-averse policies when $\eta < 0$ and vice versa.

$$(3) \quad \rho_\eta(\tau) = \text{POW}(\eta, \tau) = \begin{cases} \tau^{\frac{1}{1+|\eta|}}, & \text{if } \eta \geq 0; \\ 1 - (1 - \tau)^{\frac{1}{1+|\eta|}}, & \text{otherwise.} \end{cases} \quad (11)$$

POW [8] produces risk-averse effect with $\eta < 0$ or risk-seeking with $\eta \geq 0$.

$$(4) \quad \rho_\eta(\tau) = \text{CVaR}(\eta, \tau) = \eta\tau. \quad (12)$$

CVaR [7] remaps τ from $[0, 1]$ to $[0, \eta]$, which is widely used in distributional RL.

3.6 Diffusion Model

As a generative model, DM introduces randomness by adding Gaussian noise K times in forward diffusion process, and then obtains new samples through denoising in reverse diffusion process [22]. Specifically, DM starts with $r \sim \mathcal{D}$ and forwards the addition of Gaussian noise. In forward process, $r^{<k>}$ means the generated sample in k -th

step ($k = 1, \dots, K$) and we have $r^{<k>} \sim \mathcal{D}_q(r^{<k>})$. By the way, $\mathcal{D}_q(r) = \mathcal{D}$. ω_k is a pre-defined variance schedule in the k -th step with $v_k = 1 - \omega_k$. For the forward diffusion chain of DM which adds Gaussian noise to r recursively [48], we have for $\omega_1 < \omega_2 < \dots < \omega_K$,

$$\mathcal{D}_q(r^{<k>} | r^{<k-1>}) = \mathcal{N}(r^{<k>}; \sqrt{1 - \omega_k} r^{<k-1>}, \omega_k), \quad (13)$$

and

$$\mathcal{D}_q(r^{<1:K>} | r) := \prod_{k=1}^K \mathcal{D}_q(r^{<k>} | r^{<k-1>}). \quad (14)$$

Unrolling the above recursion, the general term expression for $r^{<k>}$ is as follows [22]:

$$\mathcal{D}_q(r^{<k>} | r) = \mathcal{N}(r^{<k>}; \sqrt{\bar{v}_k} r, (1 - \bar{v}_k)), \quad (15)$$

where $\bar{v}_k = \prod_{i=1}^k v_i$. A reparameterization trick [22] allows for the separation of a random variable (i.e., standard Gaussian distribution) and the mean-variance parameters of a Gaussian distribution, with the latter being inferred by DNNs. Consequently, (15) can be rewritten as [22]

$$r^{<k>} = \sqrt{\bar{v}_k} r + \sqrt{1 - \bar{v}_k} \bar{\epsilon}_k, \quad (16)$$

where $\bar{\epsilon}_k \sim \mathcal{N}(0, \mathbf{I})$. After K noise additions, $r^{<K>}$ approaches standard Gaussian distribution.

Reversely, the backward diffusion process predicts the Gaussian parameters (mean and variance) from $r^{<k+1>}$ to $r^{<k>}$ ($\forall k \in \{0, \dots, K-1\}$), until obtaining the generated data $r^{<0>}$. Mathematically, based on $r^{<k>}$ and r ,

$$\begin{aligned} & \mathcal{D}_q(r^{<k-1>} | r^{<k>}, r) \sim \\ & \mathcal{N}(r^{<k-1>}; \frac{1}{\sqrt{v_k}}(r^{<k>} - \frac{\omega_k}{\sqrt{1 - \bar{v}_k}} \bar{\epsilon}_k), \frac{1 - \bar{v}_{k-1}}{1 - \bar{v}_k} \omega_k). \end{aligned} \quad (17)$$

Notably, at the k -th step of the diffusion process, $\bar{\epsilon}_k$ is inferred by a DNN with parameters Θ . Therefore, by the reparameterization trick, the recursive relationship from $r^{<k>}$ to $r^{<k-1>}$ can be expressed as [22]

$$\begin{aligned} & r^{<k-1>} \leftarrow \\ & \frac{1}{\sqrt{v_k}}(r^{<k>} - \frac{\omega_k}{\sqrt{1 - \bar{v}_k}} \epsilon_\Theta(r^{<k>}, k)) + \sqrt{\frac{1 - \bar{v}_{k-1}}{1 - \bar{v}_k}} \omega_k \epsilon, \end{aligned} \quad (18)$$

where $\epsilon_\Theta(r^{<k>}, k)$ is the approximated value of $\bar{\epsilon}_k$ by DNNs and $\epsilon \sim \mathcal{N}(0, 1)$. Thus the trainable reverse diffusion chain can be optimized by the loss function as (19) on Page 7.

4 NOISE DISTRIBUTION DECOMPOSITION FOR MARL

In this section, particularly focusing on general MARL settings, we provide details of NDD toward tackling the globally shared noisy rewards with improved learning accuracy and stability. Specifically, following the idea of distributional RL, we choose the Q -value distribution (i.e., $Z_{\text{global}}^\pi(\mathbf{o}, \mathbf{a})$ in (6)) rather than the Q -value function to update agents' joint policy π . As mentioned earlier, it will also be intractable to directly decompose the distribution of the global $Z_{\text{global}}^\pi(\mathbf{o}, \mathbf{a})$. Thus, we further approximate the distribution of the global reward as a GMM [42], and propose to decompose the noisy reward distribution into

individual parts, so as to facilitate the update of local distributions. Meanwhile, to ensure the consistency between local and global Q -values, we also provide theoretical details of the distribution decomposition and present the alternative functions for distortion risk measures. Finally, DM is introduced to enhance the data of agents' buffer, and the corresponding generation and approximation errors are analyzed.

4.1 GMM-based Distributional MARL

As a parametric probability density function (PDF), a GMM represents a weighted sum of Gaussian component densities [42]. Mathematically, taking the example of any scalar x from random variable $X \sim \text{GMM}(\mu_1, \dots, \mu_N, \sigma_1^2, \dots, \sigma_N^2, w^{[1]}, \dots, w^{[N]})$, the PDF of x can be expressed as

$$\begin{aligned} & f(x; \mu_1, \dots, \mu_N, \sigma_1^2, \dots, \sigma_N^2, w^{[1]}, \dots, w^{[N]}) \\ & = \sum_{i=1}^N w^{[i]} g(x; \mu_i, \sigma_i^2), \end{aligned} \quad (20)$$

where $w^{[1]}, \dots, w^{[N]}$ are mixture weights with $\sum_{i=1}^N w^{[i]} = 1$. $g(x; \mu_i, \sigma_i^2)$ denotes the PDF of the Gaussian distribution with mean μ_i and variance σ_i^2 . Since GMM can in essence fit the shape of arbitrary distribution to describe data from single or multiple noise sources [26], \mathcal{D} can also be approximated as $\hat{\mathcal{D}}$ which follows a GMM. Thus, $\hat{\mathcal{D}}$ can be further decomposed into Gaussian components $\hat{\mathcal{D}}_i^{[1]}(\theta^{[1]}), \dots, \hat{\mathcal{D}}_i^{[N]}(\theta^{[N]})$ corresponding to different individual agents.

Without loss of generality, let $R_l^{[1]}, \dots, R_l^{[N]}$ be independent decomposed local rewards where $R_l^{[i]} \sim \hat{\mathcal{D}}_i^{[i]}(\theta^{[i]})$. We further define a function $\Psi(R_l^{[1]}, \dots, R_l^{[N]}; w^{[1]}, \dots, w^{[N]})$ to statistically combine $R_l^{[i]}$ with an assigned probability of $w^{[i]}$, and thus $\Psi(R_l^{[1]}, \dots, R_l^{[N]}; w^{[1]}, \dots, w^{[N]})$ conforms to a GMM with its expectation equaling to $\sum_{i=1}^N w^{[i]} \mathbb{E}(R_l^{[i]})$. In other words, it satisfies the additive property. Hence, the global reward R in (6) equals $\Psi(R_l^{[1]}, \dots, R_l^{[N]}; w^{[1]}, \dots, w^{[N]})$, and (6) can be rewritten as (21) on Page 8, with $\mathbb{E}[Z_{\text{global}}^\pi(\mathbf{o}, \mathbf{a})] = Q_{\text{global}}^\pi(\mathbf{o}, \mathbf{a})$, which is Q -value of the whole MAS given joint observation, action and policy $\mathbf{o}, \mathbf{a}, \pi$. Furthermore, the local Q -value distribution Z can be represented in terms of its expectation Q -value $Q_i(o^{[i]}, a^{[i]})$ as

$$Z_i^{\pi^{[i]}}(o^{[i]}, a^{[i]}) = \sum_{t=0}^{\infty} \gamma^t R_l^{[i]}(o_t^{[i]}, a_t^{[i]}). \quad (22)$$

For simplicity of representation, we might omit $\mathbf{o}, \mathbf{a}, \pi$ in $Z_{\text{global}}^\pi(\mathbf{o}, \mathbf{a})$ and $o^{[i]}, a^{[i]}, \pi^{[i]}$ in $Z_i^{\pi^{[i]}}(o^{[i]}, a^{[i]})$, and only use the notations Z_{global} and Z_i .

4.2 Consistency of Global and Local Optimal Actions

First, we show that the monotonicity constraint mentioned in Section 3.3 holds for the GMM-based distributional MARL on some conditions.

Theorem 1. For any $i = 1, \dots, N$ and Z_i defined in (22), if $w^{[i]} \geq 0$ we have

$$\frac{\partial \mathbb{E}(Z_{\text{global}})}{\partial \mathbb{E}(Z_i)} \geq 0. \quad (23)$$

$$\mathcal{L}_{\text{DM}}(\Theta) := \mathbb{E}_{k \sim \mathcal{U}(1, K), \ell \sim \mathcal{N}(0, 1), r \sim \mathcal{D}_q(r)} [\|\ell - \epsilon_{\Theta}(\sqrt{\bar{v}_k} r + \sqrt{1 - \bar{v}_k} \ell, k)\|^2] \quad (19)$$

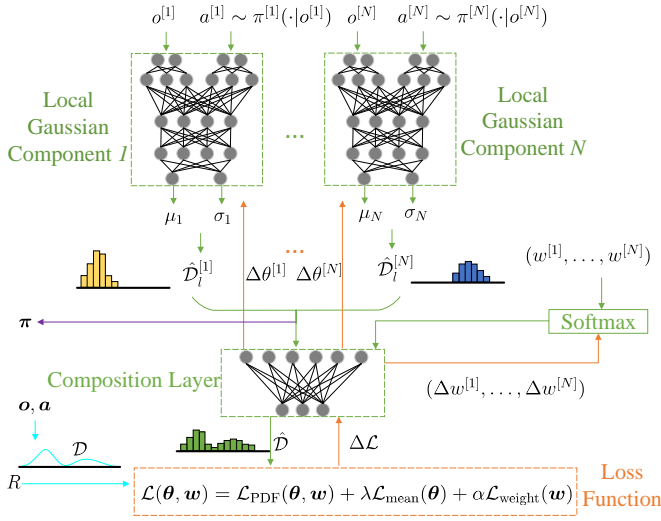


Fig. 2. Overview of the NDD algorithm.

Proof. As the definition in (21), the expectation of Z_{global} computed from M time-steps can be expressed as

$$\mathbb{E}[Z_{\text{global}}] = \text{tr}(\mathbf{W}^{\top} \mathbf{R}^{\#}), \quad (24)$$

where

$$\mathbf{W} = \begin{bmatrix} w_0^{[1]} & \dots & w_0^{[N]} \\ \vdots & \vdots & \vdots \\ w_M^{[1]} & \dots & w_M^{[N]} \end{bmatrix}, \quad (25)$$

$$\mathbf{R}^{\#} = \begin{bmatrix} \gamma^0 \mathbb{E}(R_{i,0}^{[1]}) & \dots & \gamma^0 \mathbb{E}(R_{i,0}^{[N]}) \\ \vdots & \vdots & \vdots \\ \gamma^M \mathbb{E}(R_{i,M}^{[1]}) & \dots & \gamma^M \mathbb{E}(R_{i,M}^{[N]}) \end{bmatrix}, \quad (26)$$

and $R_{i,t}^{[i]}$ is the abbreviation of $R_t^{[i]}(o_t^{[i]}, a_t^{[i]})$. Similarly, the local Z_i can be formulated as

$$[\mathbb{E}(Z_1) \dots \mathbb{E}(Z_N)] = \mathbf{1}_{(M+1) \times 1}^{\top} \mathbf{R}^{\#}. \quad (27)$$

Taking $\kappa = \min(w_t^{[i]})$, $\sum_i w_t^{[i]} = 1$ ($\forall t$) implies $0 \leq \kappa \leq \frac{1}{N}$. Therefore, (24) can be rewritten as

$$\begin{aligned} \mathbb{E}[Z_{\text{global}}] &= \text{tr}(\mathbf{W}^{\top} \mathbf{R}^{\#}) \\ &\geq \kappa \cdot \text{tr}(\mathbf{1}_{(M+1) \times N}^{\top} \mathbf{R}^{\#}) = \kappa \cdot \mathbf{1}_{(M+1) \times 1}^{\top} \mathbf{R}^{\#} \mathbf{1}_{N \times 1} \\ &= \kappa \cdot [\mathbb{E}(Z_1) \dots \mathbb{E}(Z_N)] \mathbf{1}_{N \times 1}. \end{aligned} \quad (28)$$

Consequently, (23) is satisfied as $\frac{\partial \mathbb{E}(Z_{\text{global}})}{\partial \mathbb{E}(Z_i)} \geq \kappa \geq 0$. ■

Recalling that $\mathbb{E}[Z_{\text{global}}] = Q_{\text{global}}(\mathbf{o}, \mathbf{a})$ and $\mathbb{E}[Z_i] = Q_i(o^{[i]}, a^{[i]})$, together with (2), we have the following corollary.

Corollary 1.

$$\text{argmax}_{\mathbf{a}} \mathbb{E}[Z_{\text{global}}] = \begin{pmatrix} \text{argmax}_{a^{[1]}} \mathbb{E}[Z_1] \\ \vdots \\ \text{argmax}_{a^{[N]}} \mathbb{E}[Z_N] \end{pmatrix}. \quad (29)$$

Remark: The proof of Theorem 1 implies that some excessive small weights mean trivial contributions to the group. Meanwhile, a more uniform distribution of weights can decrease the gap between $\mathbb{E}(Z_{\text{global}})$ and its lower bound. Specially, for cases where weights are evenly divided among agents (i.e., $w_i^{[i]} = \kappa = \frac{1}{N}, \forall i = 1, \dots, N$), $\mathbb{E}(Z_{\text{global}}) = \frac{1}{N} \sum_i \mathbb{E}[Z_i]$, which also satisfies (23). However, enforcing such strong constraint on weights will incur large error in decomposition results. Thus, it is meaningful to carefully calibrate the design of loss function by appending additional constraint terms.

4.3 Design of Distortion Risk Measure

As mentioned before, distortion risk function $\rho_{\eta}(\tau)$ enhances the applicability and flexibility of distributional RL. However, for MARL, $\rho_{\eta}(\tau)$ needs to be subjected to certain constraint in order to ensure that the distorted Q -value function also satisfies the monotonicity constraint in Theorem 1.

Theorem 2. Given $\frac{\partial \mathbb{E}(Z_{\text{global}})}{\partial \mathbb{E}(Z_i)} \geq 0$, if $\rho_{\eta}(\tau) \in (0, +\infty)$ ($\forall \tau$) we have

$$\frac{\partial \mathbb{E}(Z_{\text{global}, \rho})}{\partial \mathbb{E}(Z_{i, \rho})} \geq 0. \quad (30)$$

Here $Z_{\text{global}, \rho}$ and $Z_{i, \rho}$ represent that Z_{global}, Z_i have undergone the remap distortion $\rho_{\eta}(\tau)$.

Proof. According to (8),

$$\begin{aligned} \frac{\partial \mathbb{E}(Z_{\text{global}, \rho})}{\partial \mathbb{E}(Z_{i, \rho})} &= \frac{\partial \left\{ \int z d\rho_{\eta}[F_{\text{global}}(z)] \right\}}{\partial \left\{ \int z d\rho_{\eta}[F_i(z)] \right\}} \\ &= \frac{\partial \left[\int z \rho_{\eta}(\tau_{\text{global}}) dF_{\text{global}}(z) \right]}{\partial \left[\int z \rho_{\eta}(\tau_i) dF_i(z) \right]}, \end{aligned} \quad (31)$$

where F_{global}, F_i denote the CDFs of Z_{global}, Z_i ; and $\tau_{\text{global}}, \tau_i$ are their quantiles, respectively. Based on the positive-bound assumption of $\rho_{\eta}(\tau)$ ($\forall \tau$), let $\rho'_{\eta}(\tau) \in [\rho'_{\min}, \rho'_{\max}]$, (31) can be rewritten as

$$\begin{aligned} \frac{\partial \mathbb{E}(Z_{\text{global}, \rho})}{\partial \mathbb{E}(Z_{i, \rho})} &\geq \frac{\rho'_{\min}}{\rho'_{\max}} \frac{\partial \left[\int z dF_{\text{global}}(z) \right]}{\partial \left[\int z dF_i(z) \right]} \\ &= \frac{\rho'_{\min}}{\rho'_{\max}} \frac{\partial \mathbb{E}(Z_{\text{global}})}{\partial \mathbb{E}(Z_i)}. \end{aligned} \quad (32)$$

(30) holds obviously when $\rho_{\eta}(\tau) \in (0, +\infty)$. ■

Remark: Intuitively, the distortion risk measures given in Section 3.5 satisfy the condition (i.e., $\rho'_{\eta}(\tau) \in (0, +\infty)$), when they take the values in Table 7 as [8]. Furthermore,

$$\text{argmax}_{\mathbf{a}} \mathbb{E}(Z_{\text{global}, \rho}) = \begin{pmatrix} \text{argmax}_{a^{[1]}} \mathbb{E}(Z_{1, \rho}) \\ \vdots \\ \text{argmax}_{a^{[N]}} \mathbb{E}(Z_{N, \rho}) \end{pmatrix} \quad (33)$$

holds. Thus, it lays the very foundation to adopt these distortion risk measures in our case.

$$Z_{\text{global}}^{\pi}(\mathbf{o}, \mathbf{a}) = \sum_{t=0}^{\infty} \gamma^t \Psi[R_l^{[1]}(o_t^{[1]}, a_t^{[1]}), \dots, R_l^{[N]}(o_t^{[N]}, a_t^{[N]}); w_t^{[1]}, \dots, w_t^{[N]}]. \quad (21)$$

4.4 DM-based Data Augment

The Q -value distribution Z reflects more risk information than Q -value function, but the cost is an increase in the interaction between agents and the environment [1]. Especially in multi-agent scenarios, additional interaction demands several times greater than that of a single agent. Hence, using a generative model for data augmentation becomes a feasible compromise [23], [58]. Besides, in order to maintain good compatibility with GMM, DM [22] is used in our NDD, as Theorem 3 and Theorem 4 demonstrate bounded generation error and approximation error, which measure the distances between the generated sample and the original sample or the GMM, respectively.

Theorem 3 (Bounded Generation Error). *Under the assumption that $K = 25$ and $[\omega_1, \dots, \omega_K] = 0.499 \times 10^{-2} \times \frac{1}{1+e^{-h}} + 10^{-5}$, where h is an array with a length of K evenly spaced between -6 and 6 , the expectation of generation error $\mathbb{E}[(r^{<0>} - r)^2]$ satisfies*

$$\mathbb{E}[(r^{<0>} - r)^2] \lesssim (\mathbb{E}(r))^2 + 5.1359\mathbb{D}(r). \quad (34)$$

Theorem 4 (Bounded Approximation Error). *Under the assumption consistent with Theorem 3, the upper bound of approximation error expectation for $r^{<0>}$ is less than that for r , where the approximation error ξ for r is defined as the gap between r and the GMM (i.e., $r = r_{\text{GMM}} + \xi$) with $r_{\text{GMM}} \sim \text{GMM}(\cdot)$.*

We leave the proofs in Appendix A and Appendix B. Moreover, Theorem 3 and Theorem 4 imply how to select appropriate hyperparameters (e.g. diffusion steps K).

Next, we elaborate on the combination between DM and NDD. Firstly, as shown in Fig. 3 and Algorithm 1, DM is employed to learn the distribution \mathcal{D} of reward R via its sample r and generate $r^{<0>}$, where the recursive layer adopts (18). Forward and reverse diffusion processes are introduced in Section 3.6. Afterwards, NDD approximates augmented data to GMM and decomposes it into several Gaussian components for N agents. Each agent updates its policy with distributional RL and certain distortion risk functions. The complete process is visualized in Fig. 1.

4.5 Loss Function Design

As mentioned before, the NDD networks decompose the globally shared reward into weighted individual rewards for cooperative agents by estimating the distributions of decomposed rewards. Therefore, the estimation error, which can be regarded as a gap between the approximated PDF and true PDF of the globally shared reward, shall be minimized.

Without loss of generality, let P and \hat{P} be the PDFs of the true reward distribution \mathcal{D} and the estimated one $\hat{\mathcal{D}}$ through the NDD networks respectively. Based on the Wasserstein metric in (7), the loss function for NDD as

$$\mathcal{L}_{\text{PDF}}(\boldsymbol{\theta}, \mathbf{w}) = \int_{r_{\min}}^{r_{\max}} [P(u) - \hat{P}(u; \boldsymbol{\theta})]^2 du, \quad (35)$$

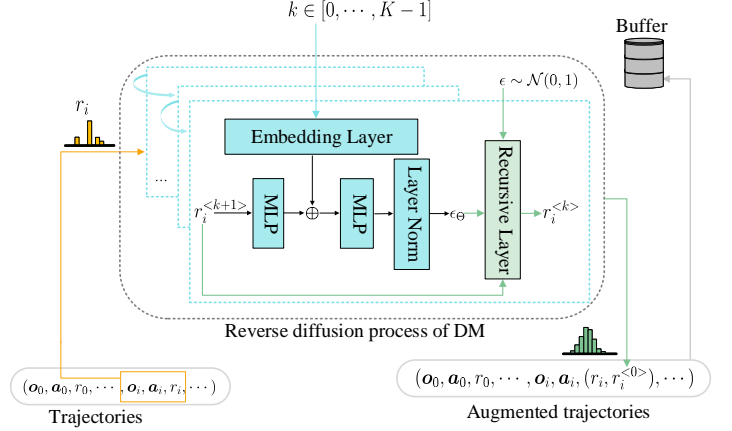


Fig. 3. Overview of the DM structure.

Algorithm 1: DM-based Data Augmentation

Input: Original reward sample r , the maximum training step T , no. of diffusion steps K , predefined hyper-parameter v_k and $\omega_k, k \in \{1, \dots, K\}$.

Output: Generated sample $r^{<0>}$.

- 1 Initialize $\Theta, t \leftarrow 0$;
- 2 **while** $t \leq T$ **do**
- 3 Randomly choose k from $\{1, \dots, K\}$;
- 4 Sample ι from $\mathcal{N}(0, 1)$;
- 5 Update Θ by minimizing (19);
- 6 **end**
- 7 Sample $r^{<K>}$ from $\mathcal{N}(0, 1)$;
- 8 **for** $k = K$ **to** 1 **do**
- 9 Infer ϵ_{Θ} based on $r^{<k>}$;
- 10 Update $r^{<k-1>}$ by $r^{<k>}$ according to (18);
- 11 **end**
- 12 **return** $r^{<0>}$.

where $[r_{\min}, r_{\max}]$ denotes the range of the reward distribution. Except the parameters Θ for DM, $\boldsymbol{\theta} = \langle \theta^{[1]}, \dots, \theta^{[N]} \rangle$ indicates all parameters of NDD networks corresponding to each agent and $\mathbf{w} = [w^{[1]}, \dots, w^{[N]}]^{\top}$. Here both $\boldsymbol{\theta}$ and \mathbf{w} are the trainable parameters in the NDD networks.

On the other hand, there may exist many possible candidates for decomposed Gaussian distributions $\hat{\mathcal{D}}_i^{[i]}(\theta^{[i]})$, $\forall i = 1, \dots, N$. To alleviate the potential issue of multiple solutions in the decomposition operation, we further impose another penalty term as

$$\mathcal{L}_{\text{mean}}(\boldsymbol{\theta}) = (\mathbf{X} - \boldsymbol{\mu} \cdot \mathbf{1}_{N \times 1})^{\top} (\mathbf{X} - \boldsymbol{\mu} \cdot \mathbf{1}_{N \times 1}). \quad (36)$$

Here $\mathbf{X} = [\mu_1(\theta^{[1]}), \dots, \mu_N(\theta^{[N]})]^{\top}$ and $\boldsymbol{\mu} = \sum_{i=1}^N \mu_i(\theta^{[i]})$, where $\mu_i(\theta^{[i]})$ denotes the mean of $\hat{\mathcal{D}}_i^{[i]}(\theta^{[i]})$.

For an individual agent, the weight represents its degree of involvement in the decomposition task. Certain excessively small weight indicates that \mathcal{L}_{PDF} has minimal supervisory impact on that component and may result in insuf-

Algorithm 2: The NDD Algorithm

Input: The global reward r , observation-action pairs $\langle o_i, a_i \rangle$ for agent $i = 1, \dots, N$, the maximum iteration number T , the error threshold e_{\min} and hyperparameters λ, α .

Output: Local Gaussian components $\hat{\mathcal{D}}_i^{[i]}$ for agent $i = 1, \dots, N$.

- 1 Initialize θ and w randomly, $t \leftarrow 0$, $e \leftarrow +\infty$;
- 2 Generate $r^{<0>}$ with Algorithm 1 when given r from \mathcal{D} ;
- 3 $r \leftarrow (r, r^{<0>})$;
- 4 **while** $t \leq T$ and $e > e_{\min}$ **do**
- 5 **for** $i = 1$ to N **do**
- 6 Generate $\mu_i(\theta^{[i]})$ and $\sigma_i(\theta^{[i]})$ of $\hat{\mathcal{D}}_i^{[i]}(\theta^{[i]})$ based on $\langle o^{[i]}, a^{[i]} \rangle$ by the local distribution network;
- 7 Calculate the Gaussian PDF $\hat{P}^{[i]}$ of $R^{[i]} \sim \hat{\mathcal{D}}_i^{[i]}(\theta^{[i]})$;
- 8 **end**
- 9 $w \leftarrow \text{Softmax}(w)$;
- 10 Concatenate the generated means as $\mathbf{X} = [\mu_1(\theta^{[1]}), \dots, \mu_N(\theta^{[N]})]^\top$;
- 11 Calculate the PDF of the estimated distribution $\hat{\mathcal{D}}$ in the form of a GMM as $\hat{P} = \sum_{i=1}^N w^{[i]} \hat{P}^{[i]}$;
- 12 Update θ and w by minimizing the loss function as in (38);
- 13 Calculate $e = \mathcal{L}_{\text{PDF}}(\theta, w)$ according to (35);
- 14 Update $t \leftarrow t + 1$;
- 15 **end**

efficient stability of the Gaussian component after decomposition. This becomes particularly evident in some simple noise scenarios, such as when the noise can be represented by the superposition of a few Gaussian components. In such cases, the remaining agents may not receive effective components. With excessively low weights, these agents might exploit extremely deviant reward distributions in training policies, ultimately affecting their performances. In addition, in order to narrow the disparity between $\mathbb{E}(Z_{\text{global}})$ and its lower bound, as mentioned in Section 4.2, weights can be aligned more evenly. Therefore, we define the corresponding penalty term as

$$\mathcal{L}_{\text{weight}}(\mathbf{w}) = \|\mathbf{w} - \frac{1}{N} \cdot \mathbf{1}_{N \times 1}\|_2. \quad (37)$$

To sum up, we obtain the Wasserstein metric-based loss function as

$$\mathcal{L}(\theta, \mathbf{w}) = \mathcal{L}_{\text{PDF}}(\theta, \mathbf{w}) + \lambda \mathcal{L}_{\text{mean}}(\theta) + \alpha \mathcal{L}_{\text{weight}}(\mathbf{w}), \quad (38)$$

where λ and α are hyperparameters.

In a nutshell, for the NDD algorithm depicted in Fig. 2, we first predict the local Gaussian components that will be utilized for local training by a multi-layer perceptron (MLP), and aggregate these decomposed ones through another MLP-based composition layer, so as to approximate the GMM along the original and augmented rewards. Finally, we update θ and w according to (38) and learn $\pi^{[i]}$ with $\hat{\mathcal{D}}_i^{[i]}(\theta^{[i]})$ through distributional RL independently. Details are summarized in Algorithm 2.

5 EXPERIMENTAL SETTINGS AND SIMULATION RESULTS

5.1 Experimental Settings

We evaluate the proposed NDD-based distributional MARL algorithm in Multi-agent Particle world Environments (MPE) and StarCraft Multi-Agent Challenge (SMAC) [33], [36], [45]. MPE is a classical MARL environment with each particle emulating the potential behaviors of one agent. Typically, MPE consists of several task-oriented collaboration scenarios (e.g., Adversary, Crypto, Speaker-Listener, Spread and Reference). Compared to MPE, SMAC is a more complicated environment for research in the field of collaborative MARL based on Blizzard’s StarCraft II RTS game, and encompasses many evaluation cases as well. Notably, as shown in Table 2, we add different types of noise to the globally shared rewards in MPE and SMAC scenarios, so as to in line with the distinct reward values (i.e., one to two orders of magnitude smaller in SMAC than MPE). Besides, the NDD approach is implemented based on PPO [46]. Additionally, we choose some typical value decomposition algorithms VDN [52], QMIX [41] as well as the current SOTA algorithm Multi-Agent PPO (MAPPO) [10], [46], [63] for comparison. Furthermore, we choose MAPPO under noiseless conditions as the Baseline to measure the performance loss of NDD and the others in noisy environments. Every method is trained with 3,000 iterations for each task in MPE, and 2×10^4 iterations for each task in SMAC. Afterwards, we compare the performance under different types of zero-mean noises, so as to rule out the possible bias impact of noise. Besides, we have $\gamma = 0.99$, $\lambda = 1$, $\alpha = 1$ and $[r_{\min}, r_{\max}] = [-10, 10]$ in our settings. As for the DM, consistent with Theorem 3 and Theorem 4, we have $K = 25$, and $[\omega_1, \dots, \omega_K] = 0.499 \times 10^{-2} \times \frac{1}{1+e^{-h}} + 10^{-5}$, where h is an array with a length of K , evenly spaced between -6 and 6 .

5.2 Performance Comparison

Fig. 4 compares NDD with the aforementioned methods and visualizes the corresponding learning process of agents for one MPE task and another SMAC task. Meanwhile, Table 3 and 4 summarize the performance comparisons in all noisy tasks. It’s worth noting that there are slight differences in the three simulations’ results of Baseline over three types of noise for each task in MPE, as the states of agents are randomly initialized at the beginning of each episode, which is in stark contrast to SMAC.

From the results, it can be clearly observed that the NDD method is significantly superior to the others, and exhibits satisfactory anti-noise effect. For example, in Reference, the interference of noise produces significant negative impact on the experimental results, especially for the value decomposition algorithms. Accordingly, it can be observed from Fig. 4 that VDN, QMIX and MAPPO fluctuate heavily and eventually converge to lower values. By the way, the effect of QMIX is much worse than other methods, due to the fact that the mixing network used in QMIX requires more stable rewards until convergence. Nevertheless, in noisy scenarios, complex mixing network yields less robust results than the one with simple summation. Hence, we

TABLE 2

Noise Configuration along Simulation Environments. It's worth noting that Noise 1 of MPE in Table 2 represents that the noise follows $\mathcal{N}(-1, 5)$ with a probability of 0.5 and $\mathcal{N}(1, 5)$ also with a probability of 0.5, instead of a simple weighted sum. Similar expressions in the following text should be interpreted accordingly.

Type	Noise 0	Noise 1	Noise 2
MPE	$\mathcal{N}(0, 5)$	$0.5\mathcal{N}(-1, 5) + 0.5\mathcal{N}(1, 5)$	$0.3\mathcal{N}(-1, 5) + 0.2\mathcal{N}(-2, 5) + 0.5\mathcal{N}(1.4, 5)$
SMAC	$\mathcal{N}(0, 0.1)$	$0.5\mathcal{N}(-0.1, 0.1) + 0.5\mathcal{N}(0.1, 0.1)$	$0.3\mathcal{N}(-0.1, 0.1) + 0.2\mathcal{N}(-0.2, 0.1) + 0.5\mathcal{N}(0.14, 0.1)$

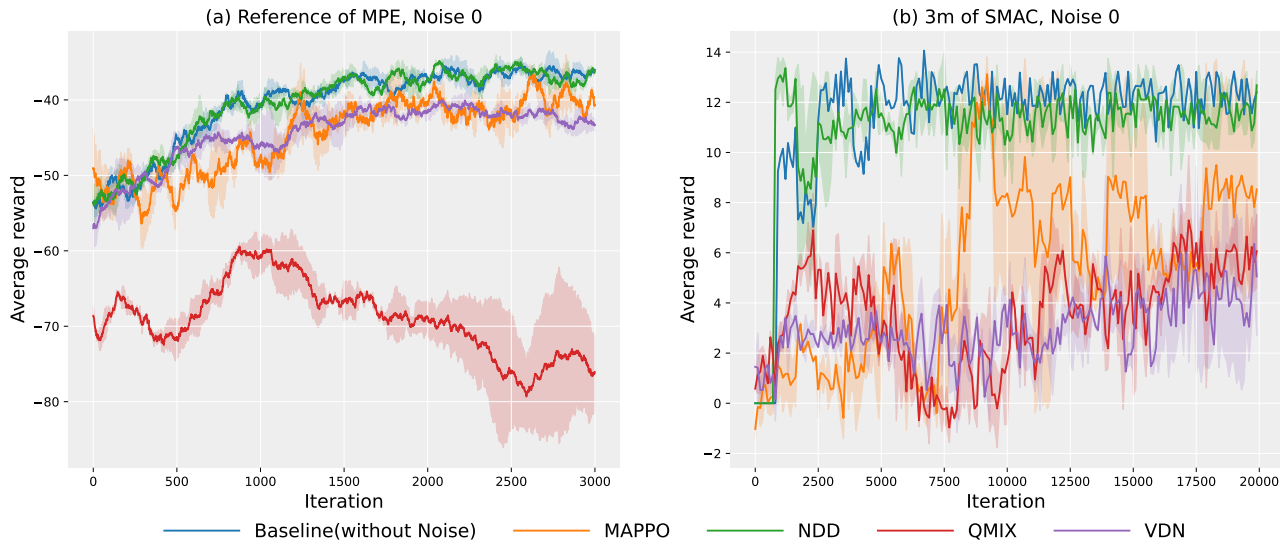


Fig. 4. Training curves about different methods. (a) shows the evaluate scores over iterations of different algorithms in the MPE Reference task with Noise 0; and (b) is in SMAC-3m task with Noise 0. Notably, the Baseline indicates the result of MAPPO under noise-free settings.

primarily choose GMM due to its simplicity and robustness. In Fig. 4, regardless of the noise distribution, the NDD method stabilizes the performance and generates results similar to noise-free tasks in most scenarios.

5.3 Distribution Decomposition Validation

We further evaluate the performance of NDD under simulated noise with arbitrary distribution. In order to further evaluate the accuracy of NDD, we decompose each noise distribution into 3 parts and summarize the related intermediate results (i.e., decomposed distributions, the corresponding weights and the computed Wasserstein distance d_p between the real and approximated distributions) in Table 5. It can be observed that though it generally leads to inferior decomposition accuracy for more complex noise distribution, all the losses are rather low in terms of Wasserstein distance (even for noise including non-Gaussian components). To make the decomposition results more intuitive, Fig. 5 compares the PDFs of two noise distributions (i.e., $0.25\beta(1, 2) + 0.75\mathcal{N}(-5, 3)$ and $0.35\mathcal{N}(-6, 1) + 0.3\beta(1, 2) + 0.35\chi(9)$) with weighted decomposed distributions, and provides the learning loss curves. It can be found from Fig. 5 that weighted distributions align closely with the noise distribution. Besides, after several hundred episodes of training, it quickly converges. In other words, the adoption of GMM to characterize the noise distribution is feasible and promising.

5.4 Results for Different Distortion Risk Measures

In order to manifest the effectiveness and stability of MARL with distortion risk functions $\rho_\eta(\tau)$, we test some formats of $\rho_\eta(\tau)$ with different parameters in Table 7 for NDD. Table 6 shows the performance of adopting different $\rho_\eta(\tau)$ in five MPE tasks, in terms of the means and standard deviations of the evaluation results. Note that means and standard deviations are compared independently. Expectation in this Table means traditional MARL which uses Q -value function to update policies.

It can be observed from Table 6 that apart from Spread, wherein the Expectation method only achieves optimal performance, most of tasks impose superior performance after imposing the risk preference on strategies. The optimal values are distributed relatively evenly among different types and parameters of $\rho_\eta(\tau)$, which reflects the significance of distributional MARL. As a function that better aligns with human decision-making habits, CPW(0.71) achieves the best results in one-third of the cases. The stability of strategy with CVaR(0.25) is the highest, at the cost of poorer performance on the effectiveness. Interestingly, some distortion risk measures are in-effective. For instance, CVaR(0.1) does not work in any of the 15 cases. In a word, CPW(0.71) can contribute to maximizing returns. Meanwhile, if stability and fault tolerance are the primary prerequisites, POW(-2) and CVaR(0.25) are worthy the recommendation.

TABLE 3
Performance of NDD and Others with Three Types of Noise in MPE Tasks.

Scenario	Type	VDN	QMIX	MAPPO	NDD	Baseline
Adversary	Noise 0	-25.63±0.78	-37.39±3.40	-8.23±0.66	-1.47±0.49	-2.39±0.22
	Noise 1	-24.24±1.13	-46.17±5.61	-6.16±0.78	-1.51±0.19	-1.91±0.35
	Noise 2	-23.72±1.57	-40.39±17.30	-7.76±0.78	-0.89±0.24	-1.82±0.10
Crypto	Noise 0	-66.97±3.03	-69.56±0.94	-28.90±1.00	-11.77±2.00	-3.68±0.97
	Noise 1	-69.11±3.29	-55.12±13.06	-22.51±0.47	-5.28±0.68	-8.67±0.63
	Noise 2	-68.29±0.38	-69.35±2.17	-24.84±1.01	-10.69±0.08	-2.43±0.13
Speaker Listener	Noise 0	-34.98±1.32	-33.66±0.86	-31.81±3.67	-33.40±1.39	-31.80±2.79
	Noise 1	-34.52±0.99	-28.75±2.42	-34.03±0.33	-29.76±0.93	-32.66±2.46
	Noise 2	-34.53±1.45	-34.06±2.19	-34.88±2.74	-32.42±0.96	-28.95±0.47
Spread	Noise 0	-104.84±0.36	-171.02±7.04	-93.58±0.68	-94.94±0.52	-91.64±0.69
	Noise 1	-98.90±0.87	-156.00±19.36	-97.86±5.23	-93.66±2.27	-94.34±0.83
	Noise 2	-97.59±1.32	-171.36±16.49	-97.91±1.05	-91.58±0.75	-92.62±0.87
Reference	Noise 0	-43.28±0.67	-76.25±4.97	-40.65±0.52	-36.33±0.35	-36.14±0.11
	Noise 1	-40.49±0.62	-58.67±9.02	-39.07±0.35	-37.44±0.92	-36.09±0.73
	Noise 2	-42.41±0.73	-62.82±10.49	-37.42±0.66	-37.29±1.54	-36.25±0.20

TABLE 4
Performance of NDD and Others with Three Types of Noise in SMAC Tasks.

Scenario	Type	VDN	QMIX	MAPPO	NDD	Baseline
3m	Noise 0	4.69±2.22	5.74±1.17	8.27±3.64	11.64±0.83	12.11±0.30
	Noise 1	5.92±1.12	6.52±1.63	8.07±2.25	11.49±1.16	
	Noise 2	4.98±2.31	2.37±0.74	11.84±1.35	8.47±1.73	
8m	Noise 0	4.55±0.75	3.39±1.60	0.42±2.51	0.48±0.49	4.98±0.40
	Noise 1	2.97±0.60	6.42±0.93	0.86±1.72	6.84±4.13	
	Noise 2	2.57±0.61	3.92±0.64	3.13±1.36	10.90±0.81	
2m vs 1z	Noise 0	2.60±0.77	2.87±0.68	3.51±0.17	3.65±0.09	3.32±0.01
	Noise 1	2.62±1.20	2.70±0.44	3.40±0.23	3.46±0.06	
	Noise 2	2.67±0.74	2.41±0.79	3.31±0.47	3.59±0.05	
2s3z	Noise 0	2.72±0.98	3.28±2.43	2.97±1.00	7.72±0.40	6.83±0.33
	Noise 1	3.11±0.63	2.29±0.61	1.52±0.33	7.21±0.46	
	Noise 2	3.36±0.69	2.02±0.47	6.51±1.75	7.49±0.29	
2s vs 1sc	Noise 0	0.14±1.22	-0.14±1.16	6.42±0.59	6.46±0.02	6.44±0.01
	Noise 1	0.37±1.22	-0.67±0.98	6.25±0.28	6.44±0.02	
	Noise 2	0.07±1.51	0.49±0.69	6.29±0.43	6.44±0.03	
3s vs 3z	Noise 0	3.20±1.46	0.91±1.64	2.76±1.84	4.79±0.16	0.00±0.00
	Noise 1	3.20±1.57	1.49±1.54	0.48±0.68	2.08±2.06	
	Noise 2	1.38±0.95	0.69±0.95	3.97±1.08	4.83±0.08	
3s vs 4z	Noise 0	2.52±1.13	3.01±0.80	0.38±1.27	2.96±0.03	2.96±0.04
	Noise 1	2.78±0.29	2.89±0.44	0.43±0.47	2.80±0.04	
	Noise 2	2.62±0.50	2.13±0.86	0.11±0.68	2.89±0.09	
3s5z	Noise 0	2.81±1.02	4.13±1.28	3.24±1.56	5.71±0.13	5.67±0.05
	Noise 1	2.77±0.27	3.38±0.46	3.69±0.75	5.27±0.37	
	Noise 2	2.89±0.42	3.91±0.85	3.24±1.04	5.75±0.24	
5m vs 6m	Noise 0	2.12±1.02	2.08±0.91	2.40±2.10	4.83±0.23	4.60±0.68
	Noise 1	2.86±0.40	3.71±0.25	2.59±2.02	2.20±2.19	
	Noise 2	3.04±0.50	3.12±0.89	2.49±0.50	2.89±0.64	
8m vs 9m	Noise 0	0.74±1.05	2.91±0.78	1.89±1.73	1.54±1.51	4.49±0.16
	Noise 1	2.43±0.24	1.64±0.48	2.72±0.68	3.57±0.18	
	Noise 2	2.12±0.42	2.00±0.64	-0.15±0.70	2.78±1.18	

TABLE 5
Modeling Accuracy of Noise Distribution Decomposition under Different GMM Assumptions. \mathcal{N} Indicates a Gaussian Distribution, while β and χ^2 Denote a Beta and a Chi-Square Distribution, Respectively.

Noise Distribution	Decomposed Gaussian Components			Weights	Wasserstein Distance d_p
	Part 1	Part 2	Part 3		
$\mathcal{N}(0, 5)$	$\mathcal{N}(5.4 \pm 0.48, 11 \pm 1.2)$	$\mathcal{N}(-0.47 \pm 0.20, 6.7 \pm 0.82)$	$\mathcal{N}(-4.4 \pm 0.14, 19 \pm 0.97)$	$[0.35 \pm 0.016, 0.30 \pm 0.029, 0.34 \pm 0.0051]$	$4.1 \pm 0.038 \times 10^{-3}$
$\mathcal{N}(0, 3)$	$\mathcal{N}(2.8 \pm 0.14, 3.3 \pm 0.25)$	$\mathcal{N}(-0.48 \pm 0.11, 2.7 \pm 0.23)$	$\mathcal{N}(-2.3 \pm 0.28, 8.2 \pm 1.4)$	$[0.30 \pm 0.029, 0.35 \pm 0.025, 0.35 \pm 0.016]$	$3.8 \pm 0.12 \times 10^{-3}$
$0.5\mathcal{N}(1, 5) + 0.5\mathcal{N}(-1, 5)$	$\mathcal{N}(4.4 \pm 2.4, 22 \pm 10)$	$\mathcal{N}(-0.10 \pm 1.4, 21 \pm 13)$	$\mathcal{N}(-2.5 \pm 1.1, 13 \pm 0.071)$	$[0.30 \pm 0.059, 0.34 \pm 0.017, 0.35 \pm 0.042]$	$3.9 \pm 0.072 \times 10^{-3}$
$0.4\mathcal{N}(5, 1) + 0.6\mathcal{N}(-5, 3)$	$\mathcal{N}(4.9 \pm 0.0030, 0.87 \pm 0.046)$	$\mathcal{N}(-3.6 \pm 0.042, 32 \pm 2.0)$	$\mathcal{N}(-5.4 \pm 0.036, 5.2 \pm 0.67)$	$[0.34 \pm 0.017, 0.30 \pm 0.059, 0.35 \pm 0.042]$	$4.1 \pm 0.74 \times 10^{-3}$
$0.25\beta(1, 2) + 0.75\mathcal{N}(-5, 3)$	$\mathcal{N}(0.29 \pm 0.10, 0.26 \pm 0.14)$	$\mathcal{N}(-4.2 \pm 0.057, 3.4 \pm 0.60)$	$\mathcal{N}(-7.0 \pm 0.27, 6.5 \pm 0.24)$	$[0.33 \pm 0.00093, 0.33 \pm 0.00047, 0.33 \pm 0.0014]$	$4.5 \pm 0.32 \times 10^{-3}$
$0.3\mathcal{N}(-1, 5) + 0.2\mathcal{N}(-2, 5) + 0.5\mathcal{N}(1.4, 5)$	$\mathcal{N}(5.9 \pm 0.32, 13 \pm 1.1)$	$\mathcal{N}(-0.19 \pm 0.31, 10 \pm 0.13)$	$\mathcal{N}(-4.0 \pm 0.20, 15 \pm 0.020)$	$[0.32 \pm 0.026, 0.33 \pm 0.0038, 0.35 \pm 0.030]$	$3.5 \pm 0.033 \times 10^{-3}$
$0.35\mathcal{N}(-6, 1) + 0.3\beta(1, 2) + 0.35\chi^2(9)$	$\mathcal{N}(9.3 \pm 0.093, 0.60 \pm 0.082)$	$\mathcal{N}(0.30 \pm 0.061, 0.19 \pm 0.062)$	$\mathcal{N}(-5.9 \pm 0.0018, 0.95 \pm 0.039)$	$[0.35 \pm 0.037, 0.32 \pm 0.026, 0.33 \pm 0.011]$	$8.8 \pm 0.64 \times 10^{-3}$

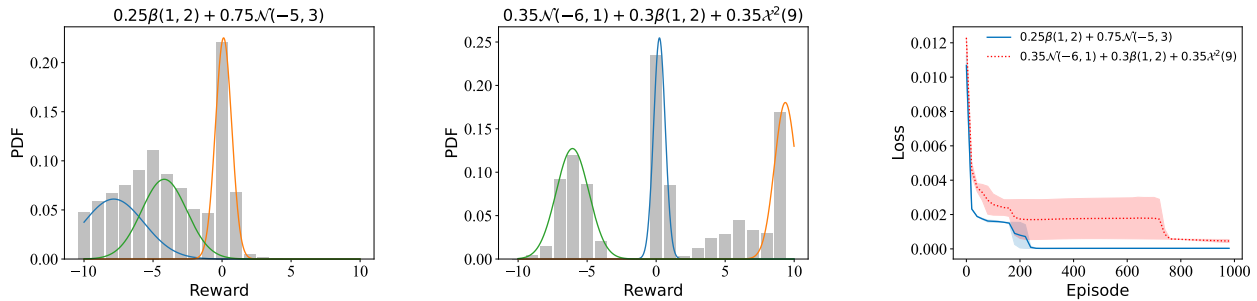


Fig. 5. Results of distribution decomposition over two noise cases (i.e., $0.25\beta(1, 2) + 0.75\mathcal{N}(-5, 3)$ and $0.35\mathcal{N}(-6, 1) + 0.3\beta(1, 2) + 0.35\chi^2(9)$). The left two sub-figures show the comparison between the practical PDF histogram and weighted PDFs of decomposed distributions (3 colored curves); while the right sub-figure shows the curve of loss function over training iterations. \mathcal{N} , β , χ^2 indicate a Gaussian, a Beta and a Chi-Square distribution, respectively.

TABLE 6
Average Scores in MPE's Tasks under Different Distortion Risk Functions.

Scenario	Type	CPW 0.71	WANG 0.75	WANG -0.75	POW -2.0	CVaR 0.25	CVaR 0.1	Expectation
Adversary	Noise 0	-0.67 ± 0.77	-11.21 ± 7.08	-2.51 ± 0.63	-4.05 ± 0.80	-1.26 ± 0.42	-4.89 ± 1.52	-1.72 ± 0.45
	Noise 1	-1.47 ± 0.63	-1.70 ± 0.61	-1.89 ± 1.06	-1.30 ± 1.89	-0.15 ± 0.35	-2.85 ± 1.16	-1.93 ± 0.43
	Noise 2	-0.86 ± 0.67	-2.23 ± 0.95	-1.31 ± 0.61	-2.61 ± 0.63	-0.78 ± 0.62	-2.98 ± 0.64	-1.35 ± 0.40
Crypto	Noise 0	-8.77 ± 6.29	-14.74 ± 0.56	-13.85 ± 1.85	-17.15 ± 0.50	-9.32 ± 1.20	-14.54 ± 1.68	-12.09 ± 1.69
	Noise 1	-8.86 ± 2.06	-14.75 ± 0.35	-9.88 ± 3.79	-10.98 ± 1.19	-10.25 ± 0.91	-11.46 ± 2.73	-5.98 ± 0.81
	Noise 2	-11.19 ± 1.83	-8.96 ± 1.58	-13.70 ± 1.90	-14.74 ± 0.49	-10.93 ± 0.64	-9.89 ± 2.54	-10.74 ± 0.52
Speaker Listener	Noise 0	-29.70 ± 1.62	-32.55 ± 2.80	-35.37 ± 1.50	-33.02 ± 1.96	-31.88 ± 3.57	-34.65 ± 2.25	-31.37 ± 1.80
	Noise 1	-31.35 ± 1.42	-34.00 ± 3.25	-32.60 ± 1.81	-34.84 ± 2.35	-32.00 ± 1.92	-36.23 ± 1.97	-30.12 ± 1.34
	Noise 2	-30.72 ± 1.78	-30.26 ± 1.31	-33.29 ± 1.84	-31.68 ± 1.44	-30.58 ± 0.96	-33.67 ± 1.04	-32.00 ± 1.35
Spread	Noise 0	-94.25 ± 1.37	-106.15 ± 2.80	-97.14 ± 2.15	-101.67 ± 3.07	-94.66 ± 1.54	-96.51 ± 1.62	-93.02 ± 0.71
	Noise 1	-94.55 ± 1.29	-102.21 ± 4.33	-99.08 ± 1.27	-99.94 ± 1.78	-95.46 ± 0.83	-94.09 ± 2.19	-93.36 ± 1.88
	Noise 2	-93.78 ± 1.98	-98.58 ± 1.81	-99.70 ± 2.08	-99.99 ± 0.75	-92.61 ± 1.64	-96.53 ± 1.70	-91.24 ± 1.58
Reference	Noise 0	-36.46 ± 0.49	-37.35 ± 1.40	-35.31 ± 1.19	-35.94 ± 1.15	-37.11 ± 0.96	-39.96 ± 1.00	-37.22 ± 0.89
	Noise 1	-35.48 ± 1.03	-36.70 ± 1.11	-37.36 ± 1.00	-36.71 ± 0.76	-36.45 ± 2.04	-37.64 ± 1.23	-36.87 ± 0.79
	Noise 2	-36.64 ± 0.93	-37.05 ± 1.16	-37.25 ± 0.90	-37.02 ± 0.84	-36.86 ± 0.79	-39.10 ± 1.17	-37.31 ± 1.33

TABLE 7
Parameters in Distortion Risk Functions.

$\rho_\eta(\tau)$	η
CPW(η, τ)	0.71
WANG(η, τ)	0.75, -0.75
POW(η, τ)	-2
CVaR(η, τ)	0.1, 0.25

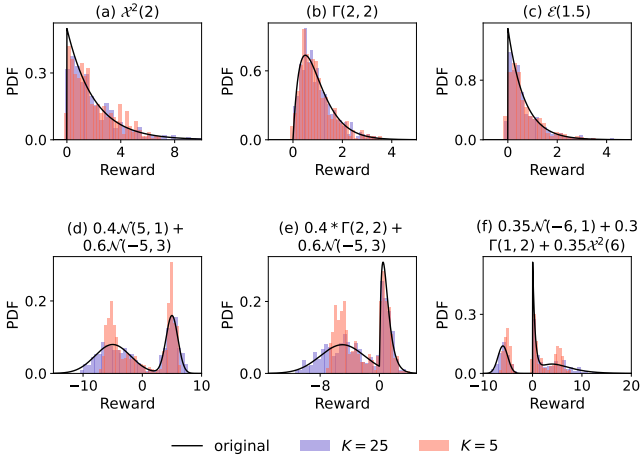


Fig. 6. The performance of DM in generated samples is illustrated. \mathcal{N} , \mathcal{X}^2 , Γ , \mathcal{E} are a Gaussian, a Chi-Square, a Gamma and an exponential distribution, respectively.

5.5 DM-based Data Augmentation

In this section, our experiments mainly focus on assessing the data preciseness provided by DM for NDD. Beforehand, we firstly evaluate the distribution of the data generated by DM and compare it with the practical distribution in Fig. 6. It can be observed that in Fig. 6 (case with $K = 25$), benefiting from the alignment capability of DM, the simulated data can resemble the original data, thus reduce the sampling and communication costs.

Next, Fig. 7 depicts the performance of the NDD approach with and without DM-based data augment. In this part, we intentionally hide some proportion of data for DM to supplement. For simplicity of representation, the ratio of the remaining data quantity to the complete one is denoted as ζ . Generally speaking, along with the increase of ζ , the NDD approach gives superior performance, consistent with our intuition. More importantly, the use of DM significantly improves the performance, strongly demonstrating the effectiveness of DM. On the other hand, for a over-small ζ , the incorporation of DM leads to a decline in the performance of NDD for some experiment scenarios, as too little data induces the significant gap between the distribution learned by DM and the original distribution. Specifically, according to analyses based on (46), the estimated expectations $\mathbb{E}(r)$ and variances $\mathbb{D}(r)$ are distorted in this data-lacking case, with non-negligible generation error. Therefore Fig. 7 also provides a good reference for balancing performance and interaction cost. Generally speaking, supplementing data within 50% from DM sounds reasonable.

6 CONCLUSION

In this paper, we propose NDD to tackle the noisy rewards during cooperative and partial observed MARL tasks. In

particular, we leverage the GMM-based reward distribution decomposition to characterize and approximate the distributional global noisy rewards by local Gaussian components, so as to mitigate the negative impact of noises. We also introduce distortion risk functions to leverage additional information learned from the Q -value distribution, and discuss their applicability. Additionally, after providing the bounded generation and approximation error, we use diffusion models for data augmentation to address the high training cost issue in distributional MARL. Moreover, we theoretically establish the consistency between the globally optimal action and locally optimal ones, and carefully calibrate the loss function designed to update NDD networks. Extensive experimental results in MPE and SMAC also prove the effectiveness and superiority of our NDD method.

APPENDIX A PROOF OF THEOREM 3

Proof. In (16), $\bar{\epsilon}_k$ is always inferred by $\epsilon_\Theta(r^{<k>}, k)$, and thus with the training loss $\xi_1(k)$ for the k -th step in DM, $\epsilon_\Theta(r^{<k>}, k)$ can be

$$\epsilon_\Theta(r^{<k>}, k) = \bar{\epsilon}_k - \xi_1(k) = \frac{r^{<k>} - \sqrt{\bar{v}_k}r}{\sqrt{1 - \bar{v}_k}} - \xi_1(k),$$

where r represents the original sample from the training dataset, which is different from the generated $r^{<0>}$ through the reverse diffusion chain. And then (18) can be rewritten as (39) where $\epsilon \sim \mathcal{N}(0, 1)$ and $k = 2, \dots, K$.

Let

$$\Gamma_1(k) = \begin{cases} \frac{1}{\sqrt{\bar{v}_k}}, & k = 1; \\ \frac{1}{\sqrt{v_k}} \frac{v_k - \bar{v}_k}{1 - \bar{v}_k}, & k = 2, \dots, K, \end{cases}$$

and

$$\Gamma_2(k) = \begin{cases} \frac{\sqrt{1 - v_k}}{\sqrt{v_k}} \epsilon, & k = 1; \\ \frac{1}{\sqrt{v_k}} \frac{1 - v_k}{1 - \bar{v}_k} (\sqrt{\bar{v}_k}r + \sqrt{1 - \bar{v}_k}\xi_1(k)) \\ \quad + \sqrt{\frac{1 - \bar{v}_{k-1}}{1 - \bar{v}_k}} \omega_k \epsilon, & k = 2, \dots, K. \end{cases}$$

We have the formula of general term as

$$r^{<0>} = r^{<K>} \prod_{i=1}^K \Gamma_1(i) + [\sum_{i=1}^K \Gamma_2(i) \prod_{j=1}^{i-1} \Gamma_1(j)] \quad (40)$$

Significantly, $\Gamma_1(k) \geq 0, \forall k = 1, \dots, K$. Let $k_{\text{exp_max}} := \text{argmax}_k (\mathbb{E}[\Gamma_2(k)])$, recalling that $r^{<K>} \sim \mathcal{N}(0, 1)$ for a sufficiently large K and $\epsilon \sim \mathcal{N}(0, 1)$, we have (41). For the same reason, if let $k_{\text{exp_min}} := \text{argmin}_k (\mathbb{E}[\Gamma_2(k)])$, we have

(42). Furthermore, (43) holds, where $\xi_{1, \text{rel}}(k) = \frac{\xi_1(k)}{\mathbb{E}(r)}$ means the relative error in the k -th step of the diffusion process.

Similarly for the variance, let $\text{argmax}_k (\mathbb{D}[\Gamma_2(k)]) = k_{\text{var_max}}$, we have (44). And according to (43) and (44), (45) is confirmed.

Based on our settings in section 5.1, we have $\sum_{i=1}^K \prod_{j=1}^{i-1} \Gamma_1(j) \approx 2.0337$ and $\prod_{i=1}^K \Gamma_1(i) \approx 3.5590 \times 10^{-4}$, as well as the expected error between the generated samples and original samples as

$$\mathbb{E}[(r^{<0>} - r)^2]$$

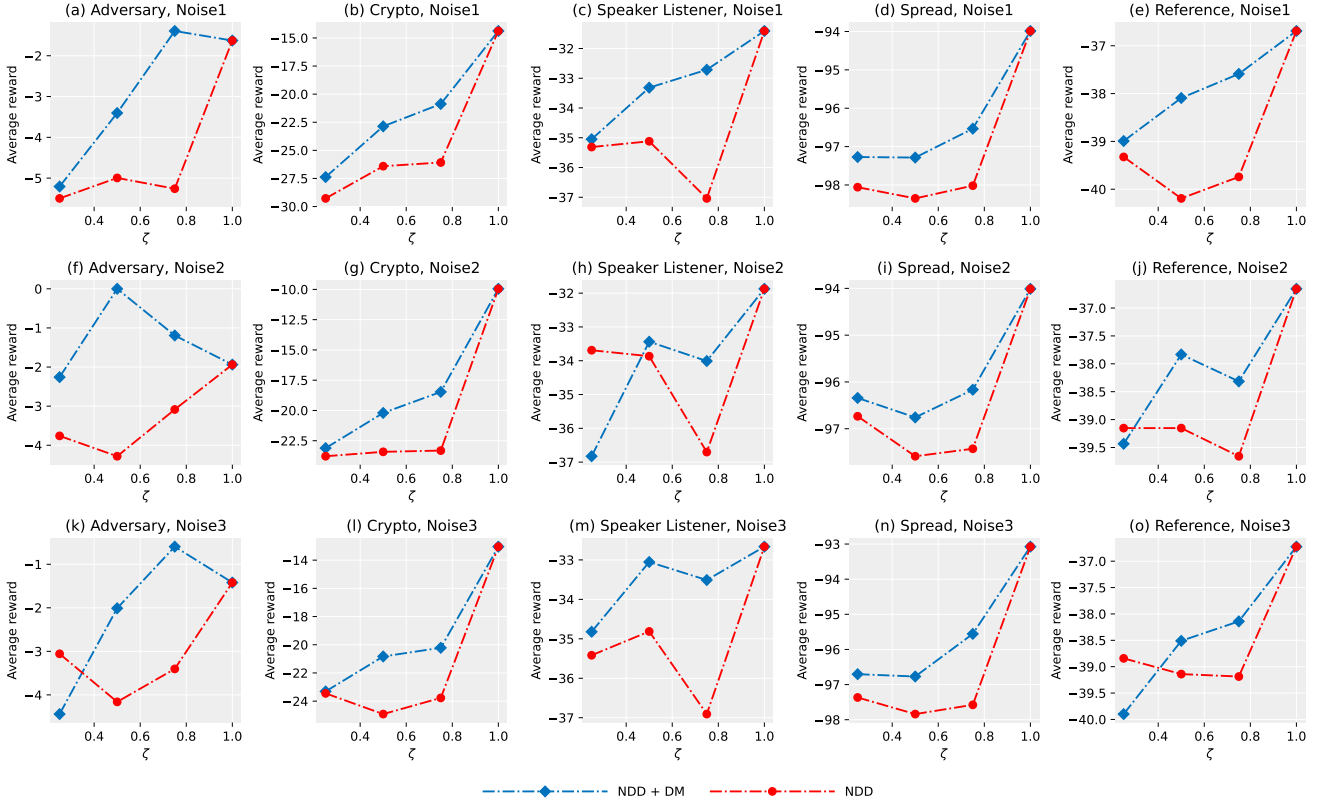


Fig. 7. The performance comparison of the NDD algorithm before and after using DM.

$$\begin{aligned}
 r^{<k-1>} &= \frac{1}{\sqrt{v_k}} \left[r^{<k>} - \frac{1 - v_k}{1 - \bar{v}_k} (r^{<k>} - \sqrt{\bar{v}_k} r - \sqrt{1 - \bar{v}_k} \xi_1(k)) \right] + \sqrt{\frac{1 - \bar{v}_{k-1}}{1 - \bar{v}_k}} \omega_k \epsilon \\
 &= \frac{1}{\sqrt{v_k}} \frac{v_k - \bar{v}_k}{1 - \bar{v}_k} r^{<k>} + \frac{1}{\sqrt{v_k}} \frac{1 - v_k}{1 - \bar{v}_k} (\sqrt{\bar{v}_k} r + \sqrt{1 - \bar{v}_k} \xi_1(k)) + \sqrt{\frac{1 - \bar{v}_{k-1}}{1 - \bar{v}_k}} \omega_k \epsilon.
 \end{aligned} \tag{39}$$

$$\begin{aligned}
 &\leq \left[2.0337 \times \left(1 + 0.2466 \max(|\xi_{1,\text{rel}}(k)|) \right) - 1 \right]^2 (\mathbb{E}(r))^2 \\
 &\quad + 1.2667 \times 10^{-7} + [\mathbb{D}(r) + 0.9226 \times 4.9877 \times 10^{-3}] \\
 &\quad \times 2.0337^2 + \mathbb{D}(r) \tag{46} \\
 &\approx \left[1.0337 + 0.5016 \max(|\xi_{1,\text{rel}}(k)|) \right]^2 (\mathbb{E}(r))^2 + \\
 &\quad 5.1359 \mathbb{D}(r) + 0.01904.
 \end{aligned}$$

It's worth noting that $|\xi_{1,\text{rel}}(k)|$ is much less than 1, and 0.01904 is much less than the first two terms. Therefore, we can have the conclusion. ■

APPENDIX B PROOF OF THEOREM 4

Beforehand, we introduce the following useful lemmas.

Lemma 1. $Z = aX + bY$ obeys GMM when given $X \sim \text{GMM}(\mu_{1,1}, \dots, \mu_{1,M}, \sigma_{1,1}^2, \dots, \sigma_{1,M}^2, w_{1,1}, \dots, w_{1,M})$, $Y \sim \text{GMM}(\mu_{2,1}, \dots, \mu_{2,N}, \sigma_{2,1}^2, \dots, \sigma_{2,N}^2, w_{2,1}, \dots, w_{2,N})$ and scalar a, b .

Proof. The PDF of Z can be rewritten as (47), where $\sum_{i=1}^M \sum_{j=1}^N w_{1,i} w_{2,j} = 1$. Obviously the PDF of Z is also in the form of a GMM. ■

Specifically, Gaussian distribution is a GMM with only one component. Therefore, the linearity additivity of Gaussian distribution and GMM is given without proof.

Corollary 2. $Z = aX + bY \sim \text{GMM}(a\mu_1 + b\mu_k, \dots, a\mu_N + b\mu_k, a^2\sigma_1^2 + b^2\sigma_k^2, \dots, a^2\sigma_N^2 + b^2\sigma_k^2, w_1, \dots, w_N)$, when given $X \sim \text{GMM}(\mu_1, \dots, \mu_N, \sigma_1^2, \dots, \sigma_N^2, w_1, \dots, w_N)$, $Y \sim \mathcal{N}(\mu_k, \sigma_k^2)$ and scalar a, b .

Lemma 2. For $k \in \{0, \dots, K\}$, if $r \sim \text{GMM}(\cdot)$, $r^{<k>} \sim \text{GMM}(\cdot)$.

Proof. We prove the lemma by induction. Naturally, by the procedures in DM, $r^{<K>} \sim \mathcal{N}(0, 1)$. Afterwards, based on (39), $r^{<K-1>}$ is expressed as a linear combination of $r \sim \text{GMM}(\cdot)$ and Gaussian distributions (i.e., $r^{<K>} \sim \mathcal{N}(0, 1)$, ϵ_Θ and ϵ). Therefore $r^{<K-1>} \sim \text{GMM}(\cdot)$. Furthermore, if $k < K$, $r^{<k-1>}$ also obeys $\text{GMM}(\cdot)$, which is represented linearly by $r, r^{<k>} \sim \text{GMM}(\cdot)$ and $\epsilon_\Theta, \epsilon \sim \mathcal{N}(\cdot)$. Thus $r^{<0>} \sim \text{GMM}(\cdot)$ according to mathematical induction [16]. ■

Next, we give the proof of Theorem 4.

Proof. Theorem 1 and Corollary 2 indicate that the samples generated by DM are more inclined to satisfy GMM, as GMM and Gaussian distribution are both additive. Linear

$$\mathbb{E}(r^{<0>} - r) \leq \frac{1}{\sqrt{v_{k_{\text{exp_max}}}}} \frac{1 - v_{k_{\text{exp_max}}}}{1 - \bar{v}_{k_{\text{exp_max}}}} \left[\sum_{i=1}^K \prod_{j=1}^{i-1} \Gamma_1(j) \right] \cdot \left[\sqrt{v_{k_{\text{exp_max}}}} \mathbb{E}(r) + \sqrt{1 - \bar{v}_{k_{\text{exp_max}}}} \xi_1(k_{\text{exp_max}}) \right] - \mathbb{E}(r). \quad (41)$$

$$\mathbb{E}(r^{<0>} - r) \geq \frac{1}{\sqrt{v_{k_{\text{exp_min}}}}} \frac{1 - v_{k_{\text{exp_min}}}}{1 - \bar{v}_{k_{\text{exp_min}}}} \left[\sum_{i=1}^K \prod_{j=1}^{i-1} \Gamma_1(j) \right] \cdot \left[\sqrt{v_{k_{\text{exp_min}}}} \mathbb{E}(r) + \sqrt{1 - \bar{v}_{k_{\text{exp_min}}}} \xi_1(k_{\text{exp_min}}) \right] - \mathbb{E}(r). \quad (42)$$

$$\begin{aligned} & |\mathbb{E}(r^{<0>} - r)| \\ & \leq \max \left(\left| \frac{1}{\sqrt{v_{k_{\text{exp_max}}}}} \frac{1 - v_{k_{\text{exp_max}}}}{1 - \bar{v}_{k_{\text{exp_max}}}} \left[\sum_{i=1}^K \prod_{j=1}^{i-1} \Gamma_1(j) \right] \left[\sqrt{v_{k_{\text{exp_max}}}} + \sqrt{1 - \bar{v}_{k_{\text{exp_max}}}} \xi_{1,\text{re1}}(k_{\text{exp_max}}) \right] - 1 \right|, \left| \frac{1}{\sqrt{v_{k_{\text{exp_min}}}}} \frac{1 - v_{k_{\text{exp_min}}}}{1 - \bar{v}_{k_{\text{exp_min}}}} \left[\sum_{i=1}^K \prod_{j=1}^{i-1} \Gamma_1(j) \right] \left[\sqrt{v_{k_{\text{exp_min}}}} + \sqrt{1 - \bar{v}_{k_{\text{exp_min}}}} \xi_{1,\text{re1}}(k_{\text{exp_min}}) \right] - 1 \right| \right) \cdot |\mathbb{E}(r)|. \end{aligned} \quad (43)$$

$$\mathbb{D}(r^{<0>} - r) \leq \left[\prod_{i=1}^K \Gamma_1(i) \right]^2 + \left[\frac{\bar{v}_{k_{\text{var_max}}}}{v_{k_{\text{var_max}}}} \left(\frac{1 - v_{k_{\text{var_max}}}}{1 - \bar{v}_{k_{\text{var_max}}}} \right)^2 \cdot \mathbb{D}(r) + \frac{1 - \bar{v}_{k_{\text{var_max}}-1}}{1 - \bar{v}_{k_{\text{var_max}}}} \omega_{k_{\text{var_max}}} \right] \left[\sum_{i=1}^K \prod_{j=1}^{i-1} \Gamma_1(j) \right]^2 + \mathbb{D}(r). \quad (44)$$

$$\begin{aligned} & \mathbb{E}[(r^{<0>} - r)^2] = |\mathbb{E}(r^{<0>} - r)|^2 + \mathbb{D}(r^{<0>} - r) \\ & \leq \max \left(\left\{ \frac{1}{\sqrt{v_{k_{\text{exp_max}}}}} \frac{1 - v_{k_{\text{exp_max}}}}{1 - \bar{v}_{k_{\text{exp_max}}}} \left[\sum_{i=1}^K \prod_{j=1}^{i-1} \Gamma_1(j) \right] \left[\sqrt{v_{k_{\text{exp_max}}}} + \sqrt{1 - \bar{v}_{k_{\text{exp_max}}}} \xi_{1,\text{re1}}(k_{\text{exp_max}}) \right] - 1 \right\}^2, \right. \\ & \quad \left. \left\{ \frac{1}{\sqrt{v_{k_{\text{exp_min}}}}} \frac{1 - v_{k_{\text{exp_min}}}}{1 - \bar{v}_{k_{\text{exp_min}}}} \left[\sum_{i=1}^K \prod_{j=1}^{i-1} \Gamma_1(j) \right] \left[\sqrt{v_{k_{\text{exp_min}}}} + \sqrt{1 - \bar{v}_{k_{\text{exp_min}}}} \xi_{1,\text{re1}}(k_{\text{exp_min}}) \right] - 1 \right\}^2 \right) [\mathbb{E}(r)]^2 + \\ & \quad \left[\prod_{i=1}^K \Gamma_1(i) \right]^2 + \left[\frac{\bar{v}_{k_{\text{var_max}}}}{v_{k_{\text{var_max}}}} \left(\frac{1 - v_{k_{\text{var_max}}}}{1 - \bar{v}_{k_{\text{var_max}}}} \right)^2 \mathbb{D}(r) + \frac{1 - \bar{v}_{k_{\text{var_max}}-1}}{1 - \bar{v}_{k_{\text{var_max}}}} \omega_{k_{\text{var_max}}} \right] \left[\sum_{i=1}^K \prod_{j=1}^{i-1} \Gamma_1(j) \right]^2 + \mathbb{D}(r). \end{aligned} \quad (45)$$

$$\begin{aligned} & f_Z(z) \\ & = \frac{1}{b} \int_{-\infty}^{+\infty} f(x; \mu_{1,1}, \dots, \mu_{1,M}, \sigma_{1,1}^2, \dots, \sigma_{1,M}^2, w_{1,1}, \dots, w_{1,M}) f\left(\frac{z - ax}{b}; \mu_{2,1}, \dots, \mu_{2,N}, \sigma_{2,1}^2, \dots, \sigma_{2,N}^2, w_{2,1}, \dots, w_{2,N}\right) dx \\ & = \frac{1}{b} \int_{-\infty}^{+\infty} \sum_{i=1}^M w_{1,i} g(x; \mu_{1,i}, \sigma_{1,i}^2) \sum_{j=1}^N w_{2,j} g\left(\frac{z - ax}{b}; \mu_{2,j}, \sigma_{2,j}^2\right) dx \\ & = \frac{1}{b} \sum_{i=1}^M \sum_{j=1}^N w_{1,i} w_{2,j} \int_{-\infty}^{+\infty} g(x; \mu_{1,i}, \sigma_{1,i}^2) g\left(\frac{z - ax}{b}; \mu_{2,j}, \sigma_{2,j}^2\right) dx \\ & = \sum_{i=1}^M \sum_{j=1}^N w_{1,i} w_{2,j} g(x; a\mu_{1,i} + b\mu_{2,j}, a^2\sigma_{1,i}^2 + b^2\sigma_{2,j}^2). \end{aligned} \quad (47)$$

additivity ensures that the approximation error between \mathcal{D} and GMM does not further expand along with diffusion process. The expected upper limit of this approximation error will be quantified below.

As there might exist a bounded approximation error ξ for $r \sim \text{GMM}(\cdot)$, we have $r = r_{\text{GMM}} + \xi$, where $r_{\text{GMM}} \sim \text{GMM}(\cdot)$, $r \sim \mathcal{D}$. Let

$$\Gamma_{2,1}(k) = \begin{cases} \frac{\sqrt{1-v_k}}{\sqrt{v_k}} \epsilon, & k = 1; \\ \frac{1}{\sqrt{v_k}} \frac{1-v_k}{1-\bar{v}_k} \left(\sqrt{\bar{v}_k} r_{\text{GMM}} + \sqrt{1-\bar{v}_k} \xi_1(k) \right) + \sqrt{\frac{1-\bar{v}_k-1}{1-\bar{v}_k}} \omega_k \epsilon, & k = 2, \dots, K, \end{cases}$$

and

$$\Gamma_{2,2}(k) = \begin{cases} 0, & k = 1; \\ \frac{1}{\sqrt{v_k}} \frac{1-v_k}{1-\bar{v}_k} \sqrt{\bar{v}_k} \xi, & k = 2, \dots, K, \end{cases}$$

we have $\Gamma_2(k) = \Gamma_{2,1}(k) + \Gamma_{2,2}(k)$. According to (40), we have (47) on Page 16.

Based on Lemma 1, Corollary 2, and Lemma 2, $r_1^{<0>} + r_2^{<0>} \sim \text{GMM}(\cdot)$. Meanwhile, $r_3^{<0>}$ resembles the approximation error for $r^{<0>}$. On condition of the aforementioned settings,

$$\mathbb{E}(r_3^{<0>}) \leq 0.9997\mathbb{E}(\xi),$$

when $K = 25$. This means, the expected approximation error for sample generated by DM will be less than that for the original sample. ■

Remark: When K is smaller, expected approximation error for generated sample will be more close to that for original one. But the condition for the reverse diffusion process in DM is $\mathcal{D}_p(r^{<K>}) \sim \mathcal{N}(0, 1)$ given $K \rightarrow +\infty$. If K is too small, the difference between $\mathcal{D}_p(r^{<K>})$ and standard Gaussian distribution is too large, which can lead to a decrease in the accuracy of the generated data. Especially in complex multi-source noise, generation error tends to amplify as shown in Fig. 6 when $K = 5$. Considering such a trade-off problem, we set $K = 25$ in our experiments.

$$r^{<0>} = \underbrace{r^{<K>} \prod_{i=1}^K \Gamma_1(i)}_{r_1^{<0>}} + \underbrace{\left[\sum_{i=1}^K \Gamma_{2,1}(i) \prod_{j=1}^{i-1} \Gamma_1(j) \right]}_{r_2^{<0>}} + \underbrace{\left[\sum_{i=1}^K \Gamma_{2,2}(i) \prod_{j=1}^{i-1} \Gamma_1(j) \right]}_{r_3^{<0>}}. \quad (47)$$

REFERENCES

- [1] Marc G Bellemare, Will Dabney, and Rémi Munos. A distributional perspective on reinforcement learning. In *Proc. Int. Conf. Mach. Learn.*, Sydney, Australia, August 2017.
- [2] Richard E Bellman and Stuart E Dreyfus. *Applied dynamic programming*, volume 2050. Princeton University Press, 2015.
- [3] Peter J Bickel and David A Freedman. Some asymptotic theory for the bootstrap. *Annals of Statistics*, 9(6):1196–1217, 1981.
- [4] Yoni Birman, Shaked Hindi, Gilad Katz, and Asaf Shabtai. Cost-effective ensemble models selection using deep reinforcement learning. *Inf. Fusion*, 77:133–148, 2022.
- [5] Lucian Buşoniu, Robert Babuška, and Bart De Schutter. Multi-agent reinforcement learning: An overview. *Innovations in Multi-Agent Systems and Applications (Studies in Computational Intelligence)*, pages 183–221, 2010.
- [6] Alvaro Ovalle Castaneda. Deep reinforcement learning variants of multi-agent learning algorithms. *Edinburgh: School of Informatics, University of Edinburgh*, 2016.
- [7] Yinlam Chow and Mohammad Ghavamzadeh. Algorithms for cvar optimization in mdps. In *Proc. Adv. Neural Inf. Process. Syst.*, Long Beach Convention Center, Long Beach, Dec. 2014.
- [8] Will Dabney, Georg Ostrovski, David Silver, and Rémi Munos. Implicit quantile networks for distributional reinforcement learning. In *Proc. Int. Conf. Mach. Learn.*, Stockholmssmässan, Stockholm Sweden, July 2018.
- [9] Will Dabney, Mark Rowland, Marc Bellemare, and Rémi Munos. Distributional reinforcement learning with quantile regression. In *Proc. AAAI Conf. Artif. Intell.*, New Orleans, Louisiana, USA, February 2018.
- [10] Christian Schroeder de Witt, Tarun Gupta, Denys Makoviichuk, Viktor Makoviyuchuk, Philip HS Torr, Mingfei Sun, and Shimon Whiteson. Is independent learning all you need in the starcraft multi-agent challenge? *arXiv:2011.09533*, 2020.
- [11] Arthur P Dempster, Nan M Laird, and Donald B Rubin. Maximum likelihood from incomplete data via the em algorithm. *J. R. Stat. Soc. B*, 39(1):1–22, 1977.
- [12] Prafulla Dhariwal and Alexander Nichol. Diffusion models beat gans on image synthesis. In *Proc. Adv. Neural Inf. Process. Syst.*, Virtual Edition, Dec. 2021.
- [13] Elhadji Amadou Oury Diallo, Ayumi Sugiyama, and Toshiharu Sugawara. Learning to coordinate with deep reinforcement learning in doubles pong game. In *Proc. 16th IEEE Int. Conf. Mach. Learn. Appl. (ICMLA)*, Cancun, Mexico, December 2017.
- [14] Ali Dorri, Salil S. Kanhere, and Raja Jurdak. Multi-agent systems: A survey. *IEEE Access*, 6:28573–28593, 2018.
- [15] Yuqing Du, Olivia Watkins, Zihan Wang, Cédric Colas, Trevor Darrell, Pieter Abbeel, Abhishek Gupta, and Jacob Andreas. Guiding pretraining in reinforcement learning with large language models. *arXiv preprint arXiv:2302.06692*, 2023.
- [16] Ed Dubinsky. Teaching mathematical induction ii. *J. Math. Behav.*, 8(3):285–304, 1989.
- [17] Jakob Foerster, Ioannis Alexandros Assael, Nando De Freitas, and Shimon Whiteson. Learning to communicate with deep multi-agent reinforcement learning. In *Proc. Adv. Neural Inf. Process. Syst.*, Barcelona Spain, December 2016.
- [18] Ana Galindo-Serrano and Lorenza Giupponi. Distributed q-learning for aggregated interference control in cognitive radio networks. *IEEE Trans. Veh. Technol.*, 59(4):1823–1834, 2010.
- [19] Jinkun Geng, Xiubo Liang, Hongzhi Wang, and Yu Zhao. Diffusion policies as multi-agent reinforcement learning strategies. In *International Conference on Artificial Neural Networks*, Heraklion city, Greece, September 2023.
- [20] Haoran He, Chenjia Bai, Kang Xu, Zhuoran Yang, Weinan Zhang, Dong Wang, Bin Zhao, and Xuelong Li. Diffusion model is an effective planner and data synthesizer for multi-task reinforcement learning. In *arXiv:2305.18459*, May 2023.
- [21] Peter Henderson, Riashat Islam, Philip Bachman, Joelle Pineau, Doina Precup, and David Meger. Deep reinforcement learning that matters. In *Proc. AAAI Conf. Artif. Intell.*, New Orleans, Louisiana, USA, February 2018.
- [22] Jonathan Ho, Ajay Jain, and Pieter Abbeel. Denoising diffusion probabilistic models. In *Proc. Adv. Neural Inf. Process. Syst.*, Virtual Edition, Dec. 2020.
- [23] Blair Hu, Ann M. Simon, and Levi Hargrove. Deep generative models with data augmentation to learn robust representations of movement intention for powered leg prostheses. *IEEE Trans. Med. Rob. Bionics*, 1(4):267–278, 2019.
- [24] Jifeng Hu, Yanchao Sun, Hechang Chen, Sili Huang, Yi Chang, Lichao Sun, et al. Distributional reward estimation for effective multi-agent deep reinforcement learning. In *Proc. Adv. Neural Inf. Process. Syst.*, Virtual Edition, November/December 2022.
- [25] Maximilian Hüttenrauch, Adrian Šošić, and Gerhard Neumann. Guided deep reinforcement learning for swarm systems. *arXiv:1709.06011*, 2017.
- [26] Nobutaka Ito, Christopher Schymura, Shoko Araki, and Tomohiro Nakatani. Noisy cgmm: Complex gaussian mixture model with non-sparse noise model for joint source separation and denoising. In *Proc. EUSIPCO*, Sep 2018.
- [27] Yinsen Jia, Xinqi Tu, and Wei Yan. An uav wireless communication noise suppression method based on ofdm modulation and demodulation. *Radio Sci.*, 55(2):1–14, 2020.
- [28] Ozsel Kilinc and Giovanni Montana. Multi-agent deep reinforcement learning with extremely noisy observations. *arXiv:1812.00922*, 2018.
- [29] Guillaume Lample and Devendra Singh Chaplot. Playing fps games with deep reinforcement learning. In *Proc. AAAI Conf. Artif. Intell.*, San Francisco, California USA, February 2017.
- [30] Yann LeCun, Yoshua Bengio, and Geoffrey Hinton. Deep learning. *Nature*, 521(7553):436–444, 2015.
- [31] Zhuoran Li, Ling Pan, and Longbo Huang. Beyond conservatism: Diffusion policies in offline multi-agent reinforcement learning. *arXiv preprint arXiv:2307.01472*, 2023.
- [32] Michael L. Littman. Markov games as a framework for multi-agent reinforcement learning. In William W. Cohen and Haym Hirsh, editors, *Proc. 11th Int. Conf. Mach. Learn.*, pages 157–163. Morgan Kaufmann, San Francisco (CA), 1994.
- [33] Ryan Lowe, Yi I Wu, Aviv Tamar, Jean Harb, OpenAI Pieter Abbeel, and Igor Mordatch. Multi-agent actor-critic for mixed cooperative-competitive environments. In *Proc. Adv. Neural Inf. Process. Syst.*, Long Beach, California, USA, December 2017.
- [34] Ishai Menache, Shie Mannor, and Nahum Shimkin. Basis function adaptation in temporal difference reinforcement learning. *Ann. Oper. Res.*, 134:215–238, 2005.
- [35] Volodymyr Mnih, Koray Kavukcuoglu, David Silver, Alex Graves, Ioannis Antonoglou, Daan Wierstra, and Martin Riedmiller. Playing atari with deep reinforcement learning. *arXiv preprint arXiv:1312.5602*, 2013.
- [36] Igor Mordatch and Pieter Abbeel. Emergence of grounded compositional language in multi-agent populations. In *Proc. AAAI Conf. Artif. Intell.*, New Orleans, Louisiana, USA, February 2018.
- [37] A. Nichol, P. Dhariwal, and A. Ramesh. Glide: Towards photorealistic image generation and editing with text-guided diffusion models. In *arXiv:2112.10741*, Mar. 2021.
- [38] Frans A Oliehoek and Christopher Amato. *A concise introduction to decentralized POMDPs*. Springer, 2016.
- [39] Aditya Ramesh, Prafulla Dhariwal, and Alex Nichol. Hierarchical text-conditional image generation with clip latents. In *arXiv:2204.06125*, Apr. 2022.
- [40] Tabish Rashid, Gregory Farquhar, Bei Peng, and Shimon Whiteson. Weighted qmix: Expanding monotonic value function factorisation for deep multi-agent reinforcement learning. In *Proc. Adv. Neural Inf. Process. Syst.*, Virtual Edition, December 2020.
- [41] Tabish Rashid, Mikayel Samvelyan, Christian Schroeder De Witt, Gregory Farquhar, Jakob Foerster, and Shimon Whiteson. Monotonic value function factorisation for deep multi-agent reinforcement learning. *Proc. Conf. Mach. Learn.*, 21(1):7234–7284, 2020.
- [42] Douglas Reynolds. Gaussian mixture models. *Encyclopedia of Biometrics*, 741(659-663), 2009.

- [43] Yossi Rubner, Carlo Tomasi, and Leonidas J Guibas. The earth mover's distance as a metric for image retrieval. *Int. J. Comput. Vision*, 40(2):99, 2000.
- [44] Chitwan Saharia, William Chan, Huiwen Chang, Chris Lee, Jonathan Ho, Tim Salimans, David Fleet, and Mohammad Norouzi. Palette: Image-to-image diffusion models. In *n Proc. ACM SIGGRAPH Conf.*, Vancouver BC Canada, Aug. 2022.
- [45] Mikayel Samvelyan, Tabish Rashid, Christian Schroeder de Witt, Gregory Farquhar, Nantas Nardelli, Tim G. J. Rudner, Chia-Man Hung, Philip H. S. Torr, Jakob Foerster, and Shimon Whiteson. The StarCraft Multi-Agent Challenge. *CoRR*, abs/1902.04043, 2019.
- [46] John Schulman, Filip Wolski, Prafulla Dhariwal, Alec Radford, and Oleg Klimov. Proximal policy optimization algorithms. *arXiv:1707.06347*, 2017.
- [47] Bharat Singh, Rajesh Kumar, and Vinay Pratap Singh. Reinforcement learning in robotic applications: a comprehensive survey. *Artif. Intell. Rev.*, 55:945–990, April 2021.
- [48] Jascha Sohl-Dickstein, Eric Weiss, Niru Maheswaranathan, and Surya Ganguli. Deep unsupervised learning using nonequilibrium thermodynamics. In *Proc. Int. Conf. Mach. Learn.*, Lille, France, Jul 2015.
- [49] Kyunghwan Son, Daewoo Kim, Wan Ju Kang, David Earl Hostallero, and Yung Yi. Qtran: Learning to factorize with transformation for cooperative multi-agent reinforcement learning. In *Proc. Int. Conf. Mach. Learn.*, Long Beach, California, USA, June 2019.
- [50] Sainbayar Sukhbaatar, Rob Fergus, et al. Learning multiagent communication with backpropagation. In *Proc. Adv. Neural Inf. Process. Syst.*, Barcelona Spain, December 2016.
- [51] Wei-Fang Sun, Cheng-Kuang Lee, and Chun-Yi Lee. Dfac framework: Factorizing the value function via quantile mixture for multi-agent distributional q-learning. In *Proc. ICML*, Virtual Edition, July 2021.
- [52] Peter Sunehag, Guy Lever, Audrunas Gruslys, Wojciech Marian Czarnecki, Vinicius Zambaldi, Max Jaderberg, Marc Lanctot, Nicolas Sonnerat, Joel Z Leibo, Karl Tuyls, et al. Value-decomposition networks for cooperative multi-agent learning. *arXiv:1706.05296*, 2017.
- [53] Richard S Sutton, Andrew G Barto, et al. *Introduction to reinforcement learning*, volume 135. MIT Press, 1998.
- [54] A. Tversky and D. Kahneman. Advances in prospect theory: Cumulative representation of uncertainty. *J. Risk Uncertainty*, 5(4):297–323, Oct. 1992.
- [55] Huiwei Wang, Xiaofeng Liao, Tingwen Huang, and Chaojie Li. Cooperative distributed optimization in multiagent networks with delays. *IEEE Trans. Syst. Man Cybern.: Syst.*, 45(2):363–369, 2015.
- [56] Jing kang Wang, Yang Liu, and Bo Li. Reinforcement learning with perturbed rewards. In *Proc. AAAI Conf. Artif. Intell.*, New York, USA, feb 2020.
- [57] Shaun S. Wang. A class of distortion operators for pricing financial and insurance risks. *J. Risk Insurance*, 67(1):15–36, Mar. 2000.
- [58] Shuai Wang, Yexin Yang, Zhanghao Wu, Yanmin Qian, and Kai Yu. Data augmentation using deep generative models for embedding based speaker recognition. *IEEE/ACM Transactions on Audio, Speech, and Language Processing*, 28:2598–2609, 2020.
- [59] Ying Wang and Clarence W De Silva. Multi-robot box-pushing: Single-agent q-learning vs. team q-learning. In *Proc. of IROS*, Beijing, China, 2006.
- [60] Zhendong Wang, Jonathan J Hunt, and Mingyuan Zhou. Diffusion policies as an expressive policy class for offline reinforcement learning. In *arXiv:2208.06193*, Aug. 2023.
- [61] George Wu and Richard Gonzalez. Curvature of the probability weighting function. *Manage. Sci.*, 42(12):1676–1690, 1996.
- [62] Feng Xiao and Long Wang. Asynchronous consensus in continuous-time multi-agent systems with switching topology and time-varying delays. *IEEE Trans. Autom. Control*, 53(8):1804–1816, 2008.
- [63] Chao Yu, Akash Velu, Eugene Vinitsky, Jiaxuan Gao, Yu Wang, Alexandre Bayen, and Yi Wu. The surprising effectiveness of ppo in cooperative multi-agent games. In *Proc. Adv. Neural Inf. Process. Syst.*, Virtual Edition, November/December 2022.